

# Magmatic Evolution of the Skye Igneous Centre, Western Scotland: Modelling of Assimilation, Recharge and Fractional Crystallization

SARAH J. FOWLER<sup>1\*</sup>, WENDY A. BOHRSON<sup>1</sup> AND FRANK J. SPERA<sup>2</sup>

<sup>1</sup>DEPARTMENT OF GEOLOGICAL SCIENCES, CENTRAL WASHINGTON UNIVERSITY, ELLENSBURG, WA 98926, USA

<sup>2</sup>DEPARTMENT OF GEOLOGICAL SCIENCES AND INSTITUTE FOR CRUSTAL STUDIES, UNIVERSITY OF CALIFORNIA, SANTA BARBARA, SANTA BARBARA, CA 93106, USA

RECEIVED SEPTEMBER 1, 2003; ACCEPTED AUGUST 30, 2004  
ADVANCE ACCESS PUBLICATION NOVEMBER 4, 2004

*The Skye igneous centre, forming part of the British Tertiary magmatic province, developed over a ~7 Myr period (61–54 Ma) and is characterized by a complex suite of lavas, hypabyssal and intrusive rocks of picritic to granitic composition. The intrusion of magma from mantle to crust at  $\sim 2 \times 10^{-3} \text{ km}^3/\text{yr}$  (6 Mt/yr) advected magmatic heat of roughly 0.2 GW averaged over the period of magmatism supporting an ‘excess’ heat flux of about  $130 \text{ mW}/\text{m}^2$ , or about twice the present-day average continental heat flow. The volume of new crust generated at Skye ( $\sim 15\,000 \text{ km}^3$ ) spread over the present-day area of Skye corresponds to  $\sim 9 \text{ km}$  of new crust. The geochemical evolution of the Skye magmatic system is constrained using the Energy-Constrained Recharge, Assimilation, and Fractional Crystallization (EC-RAFC) model to understand variations in the Sr- and Pb-isotopic and Sr trace-element composition of the exposed magmatic rocks with time. The character (composition and specific enthalpy) of both assimilant and recharge magma appears to change systematically up-section, suggesting that the magma reservoirs migrated to progressively shallower levels as the system matured. The model of the magma transport system that emerges is one in which magma batches are stored initially at lower-crustal levels, where they undergo RAFC evolution. Residual magma from this stage then migrates to shallower levels, where mid-crustal wall rock is assimilated; the recharge magma at this level is characterized by an increasingly crustal signature. For some of the stratigraphically youngest rocks, the data suggest that the magma reservoirs ascended into, and interacted with, upper-crustal Torridonian metasediments.*

KEY WORDS: assimilation; EC-RAFC model; geochemical modelling; magma recharge; Skye magmatism

## INTRODUCTION

The compositional diversity of igneous rocks on Earth reflects the complex interplay between physical and chemical processes during magma generation, segregation, ascent, storage, mixing, crystallization and eruption. Bowen (1928) noted the essential connection between fractional crystallization and crustal assimilation. He recognized that the release of latent heat as a result of the cooling and crystallization of magma could, in favorable circumstances, raise wall-rock temperatures above the local solidus,  $T_s(a_i, p)$ , where  $a_i$  represents the activity of the independent chemical components and  $p$  is the pressure. Physical mobilization and subsequent addition of anatectic melt and country-rock residue to a magma body leads to chemical contamination, which can influence the course of crystallization. Significant heat transfer and magma compositional evolution occur even when no country-rock partial melting takes place, as magmatic heat removal is a requirement for crystallization and fractional crystallization changes the composition of derivative liquids as governed by the principles of phase equilibria. In addition to fractional crystallization and assimilation, the addition of new magma batches

\*Corresponding author. Present address: Department of Geological Sciences, University of California, Santa Barbara, Santa Barbara, CA 93106, USA. Telephone: (805) 893-4880. E-mail: fowler@umail.ucsb.edu.

(recharge), which often are compositionally and thermally distinct, also influences magma evolution via the process of magma mixing and, if the specific enthalpy of the recharge magma is higher than that of the magma it intrudes, by providing additional energy for country-rock heating, anatexis and possible additional contamination. A high magma recharge rate both enhances anatexis and increases the probability that wall-rock partial melts will gain access to the evolving magma. To quantify magma contamination, it is convenient to define an effective mass of country rock,  $M_a^o$ , that acts as a sink for magma-derived heat on the time-scale of magma compositional and thermal evolution ( $10^2$ – $10^6$  yr). The mass ratio of assimilated melt added to magma,  $\chi M_a^*$ , to the mass of country rock acting as a sink,  $M_a^o$ , is a convenient measure of the importance of chemical contamination. Here,  $\chi$  represents the fraction of anatectic melt generated in country rock that is added to (or contaminates) the evolving magma. The parameter  $\lambda \equiv \chi M_a^*/M_a^o$  serves as a measure to gauge the importance of magma contamination by assimilation. Similarly,  $M_r$  and  $M_c$  serve as metrics to gauge the importance of recharge and fractional crystallization, respectively. It is desirable to relate  $\lambda$ ,  $M_r$  and  $M_c$  to the chemical evolution of magma via a relationship that couples magma energetics to compositional evolution, to account for the complexities of simultaneous recharge and fractional crystallization. Trace-element concentrations and isotope ratios are especially useful petrogenetic markers. One of the outstanding challenges in igneous petrology and geochemistry is to quantify RAFC phenomena and discriminate shallow-level signatures from those imparted to the primary magma by variable degrees of melting of heterogeneous mantle sources at specific environmental conditions of  $a_i$ , pressure and temperature.

In this study, we use the Energy-Constrained Recharge, Assimilation, and Fractional Crystallization (EC-RAFC) geochemical modelling tool (Bohrson & Spera, 2001, 2003; Spera & Bohrson, 2001, 2002) to examine the complex petrologic history of a small portion of the British Tertiary Igneous Province (BTIP). Our goal is to assess quantitatively the relative importance of assimilation, recharge and fractional crystallization in the petrologic evolution of the compositionally diverse Skye Tertiary igneous centre in western Scotland. Previous workers have attributed the geochemical diversity of the Skye magmatic rocks to multiple heterogeneous mantle sources (e.g. asthenosphere, lithosphere, depleted lithosphere, etc.) along with a variety of crustal-level processes. The Skye igneous centre was chosen because it has a long history of investigation (e.g. Harker, 1904; Anderson & Dunham, 1966; Moorbath & Welke, 1969; Thompson *et al.*, 1972; Dickin, 1981; Thompson, 1982; Mussett *et al.*, 1988; Dagley *et al.*, 1990; Gibson, 1990; Emeleus & Gyopari, 1992; Scarrow, 1992; Hamilton *et al.*,

1998) and because it exhibits a complex evolution that provides a stringent test of the EC-RAFC model. Available geochemical data show unequivocal evidence for the involvement of open-system processes in the petrogenesis of intrusive and extrusive centres throughout  $\sim 7$  Myr of Skye Tertiary magmatism; the EC-RAFC model was specifically derived to accommodate open-system behaviour. Because of the complexity and protracted history of magmatism, the EC-RAFC simulator was applied sequentially to each of three distinct petrologic lineages defined on the basis of spatial relatedness, geochronology and petrological characteristics, as gleaned from the published literature. The purpose is to develop an improved quantitative understanding of the roles that shallow and deep-level processes played at Skye and to forge a link between regional-scale material and energy balances and the record preserved in exposed igneous rocks.

## THE SKYE IGNEOUS CENTRE, WESTERN SCOTLAND

The Skye igneous centre (Fig. 1) is part of the BTIP, the site of voluminous mafic to silicic magmatism in mainland western Scotland and the offshore Hebridean islands, associated with the opening of the North Atlantic Ocean (Saunders *et al.*, 1997). On Skye, the bulk of igneous activity is hypothesized to have occurred in less than 3 Myr (Chambers & Pringle, 2001), although the total duration of magmatism was  $\sim 7$  Myr. The first event was eruption of a 1.2–1.7 km thick succession of flood basalts (the Skye lavas) exposed in north and west-central Skye over an area of 1550 km<sup>2</sup> (Thompson, 1982; Emeleus, 1991; England, 1994; Williamson & Bell, 1994). The Skye Lavas dominantly consist of transitional to alkalic basalt compositions (including both *hy* and *ne* normative basalts) of the Skye Main Lava Series (SMLS). The relative depletion of heavy rare earth elements is consistent with residual garnet in the SMLS source region and hence suggests melt segregation of parental SMLS liquids from peridotitic mantle beneath relatively thick ( $\sim 80$  km) lithosphere within the stability field of garnet (Ellam, 1992; White & McKenzie, 1995). In west-central Skye, a later tholeiitic magma type, the Preshal More basalt (PMB), lies unconformably upon the volumetrically dominant SMLS and exhibits strong chemical similarity to mid-ocean ridge basalt (MORB) (Thompson, 1982). The SMLS to PMB compositional change has been interpreted as representing progressive upward movement of the region of partial melting because of lithospheric thinning during the early stages of opening of the North Atlantic basin in the Paleocene. Presumably, the transport of mantle heat by magma advection was a contributing factor to lithospheric thinning. A maximum

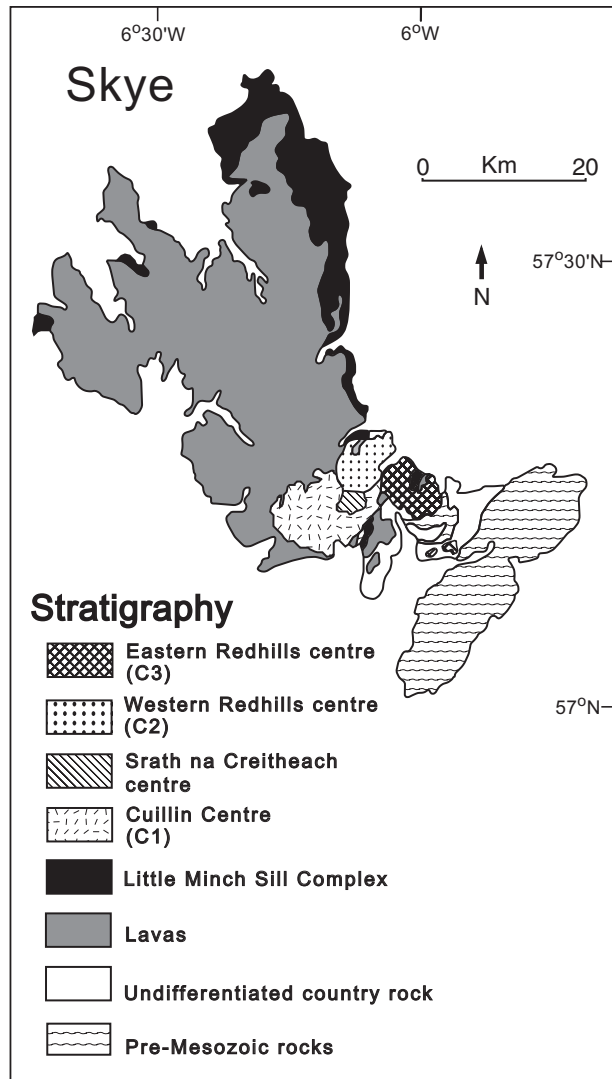


Fig. 1. Geological sketch map of the Isle of Skye, showing the Tertiary igneous rocks mentioned in the text (adapted from Emeleus & Gyopari, 1992).

age for the Skye lavas has been estimated at  $60.53 \pm 0.08$  Ma by Hamilton *et al.* (1998), based on the U–Pb zircon age of the Rum central complex. Clasts of the Rum central complex are present in conglomerates intercalated with Skye lavas in the lower portion of the lava field. Based on zircon-bearing pegmatites in gabbros of the Cuillin centre, which intrude the Skye Lavas, Hamilton *et al.* (1998) estimated an upper age limit for the Skye lavas of  $58.91 \pm 0.07$  Ma and hence a maximum duration of magmatism of  $1.6 \pm 0.3$  Myr. Jurassic sediments that underlie Skye lavas host an extensive intrusive suite, the Little Minch Sill Complex (Gibson & Jones, 1991). Intrusive relationships indicate that the sill complex is marginally younger than the Skye lavas (Gibson, 1990).

Towards the end of the period of flood basalt volcanism, a central intrusive complex developed, in which four magmatic centres, each comprising multiple intrusions, formed in succession as the focus of igneous activity moved progressively eastward. From west to east, these are the Cuillin centre, which is dominantly mafic, and the Srath na Creitheach, Western Redhills, and Eastern Redhills centres, which are dominantly granitic (e.g. Emeleus, 1982; Emeleus & Gyopari, 1992). Based on gravity data, the Cuillin centre is believed to be an approximately cylindrical mass extending to at least 16 km beneath the surface (e.g. Bott & Tucson, 1973). Although the earliest Cuillin magmas have SMLS compositions, the bulk of the centre displays a strong compositional affinity with PMB lavas. Numerous dykes of the main Skye swarm cut the SMLS and chemically are similar to PMB tholeiites, probably injected laterally from the Cuillin centre (Walker, 1993). Dickin & Exley (1981) reported an age of  $59.30 \pm 0.7$  Ma for the youngest Cuillin centre intrusion, the Coire Uaigneach Granophyre. The Srath na Creitheach centre is small and poorly documented, and is not included in this investigation. The Western and Eastern Redhills granites are approximately 2 km thick (Gouly *et al.*, 1992). The presence of hybrid bodies in the Western and Eastern Redhills centres suggests that basaltic magma (evidence of recharge) was available during the formation of the granitic centres. Further evidence of this is intrusion of mafic to intermediate cone sheets and dykes throughout the history of the central complex (Emeleus & Gyopari, 1992). Age determinations have been reported for the Loch Ainort granite of the Western Redhills centre (Table 1) ( $58.58 \pm 0.3$  Ma; Chambers & Pringle, 2001) and the Beinn an Dubhaich granite of the Eastern Redhills centre (Table 1; Outer Granite) ( $53.5 \pm 0.8$  Ma; Dickin, 1981). These relations are summarized in Table 1.

A purpose of this paper is to develop a semi-quantitative account of Skye geochemical evolution based on the fundamental processes of assimilation, magma mixing and fractional crystallization, without calling on exotic processes or special mantle sources. We use Pb- and Sr-isotope and Sr-concentration data, along with inferred crustal assimilation compositions and the melting behaviour of possible crustal contaminants, to model the relative importance of assimilation, recharge and fractional crystallization, develop first-order quantitative estimates of material budgets (i.e. relative masses of assimilation, recharge magmas and cumulates) and address the implications for the growth and differentiation of crust in the Skye province. Our goal is to connect regional-scale ‘geophysical’ estimates for crustal growth rates and heat transport summarized in the next section to the petrological evolution recorded in the composition of exposed intrusive, hypabyssal and extrusive igneous rocks at Skye.

Table 1: *The Skye Tertiary igneous centre: stratigraphy, composition, petrography and geochronology*

Stratigraphic divisions	Composition	Petrography
<i>Eastern Redhills centre (C3):</i>		
(Youngest)		
Composite (mafic to silicic) sills (may overlap in time with below) ( $55.0 \pm 0.8$ Ma)	Ferrobasalt—rhyolite	Hybrid mafic—silicic sills. Resorbed alkali feldspar xenocrysts in upper and lower margins
Inner granite $54.0 \pm 1.4$ Ma*	Dominantly granitic	
Outer granite ( $53.50 \pm 0.8$ Ma)	Dominantly granitic	
<i>Western Redhills centre (C2):</i>		
South		
Marsco granite	Dominantly granitic; ferrodiorite, gabbro present	Hybrid mafic—silicic rocks
Marscoite suite (core is ferrodiorite—contact grades to Southern Porphyritic granite)	Marscoite—Giamatgite mixed suite	Glamalg granite contains phenocrysts, mafic blebs of Marsco Summit Gabbro and felsic inclusions similar to Eastern Redhills granites
Glamalg granite	Northern Porphyritic granite Loch Ainort granite ( $58.58 \pm 0.30$ Ma)	Marscoite Suite is a ring dyke showing mixing between ferrodiorite and the Southern Porphyritic granite
Marsco Summit Gabbro	Maol na Gainmhich granite	LA xenoliths present in Marscoite Suite
<i>Srath na Creitheach center:</i>		
<i>Cullin center (C1):</i>		
Coire Uaigneich	Dominantly granitic	
Granophyre ( $59.30 \pm 0.7$ Ma)	Peridotite—granite, dominantly gabbro Granite	Partially melted sandstone xenoliths
Intrusive tholeiites	Gabbroic	
Druim na Ramh Ring Euclrite	Gabbroic	
Layered series ( $58.91 \pm 0.07$ Ma)	Gabbroic	
Border Group	Gabbroic	
Outer Unlayered Gabbro	Basalt—dolerite	Pl xenocrysts
Cone sheets, dykes (coeval with many of the above Cullins rocks)		
<i>Little Minch Sill Complex: (may overlap with the Skye lavas)</i>		
<i>Skye lavas:</i>	Picrite, picrodolerite, and crinanite units	
	Picritic basalt-trachyte, dominantly basaltic	Picritic basalt, basalt: variable of Mg-number values ( $F_{088}-F_{092}$ ). Some rounded, resorbed pl
PMB magma type (unconformable above SMLS)		
Intercalated SMLS basalts (Upper part of lava field: intercalated low-Fe intermediates and Fe-rich lavas) (Lower part of lava field: dominantly SMLS basalts and Fe-rich lavas)		
( $60.53 \pm 0.08$ Ma) Maximum age of lavas		

Data from Wager *et al.* (1953); Anderson & Dunham (1966); Thompson (1969); Thompson *et al.* (1972, 1982); Bell (1976); Dickin (1981); Dickin & Exley (1981); Dickin *et al.* (1984); Bell & Harris (1986); Dagley *et al.* (1990); Gibson & Jones (1990, 1991); Emelius (1991); Emelius & Gyopari (1992); Scarrow (1992); Bell & Pankhurst (1993); Bell *et al.* (1994); Scarrow & Cox (1995); Hamilton *et al.* (1998); Chambers & Pringle (2001). LA, Lewisian amphibolite.

\*Kilchrist Hybrids: not included in the present study.

## Magma and energy budget

Given a surface area of  $\sim 1550 \text{ km}^2$  for the Skye lavas and Little Minch Sill Complex (see Fig. 1 and Emeleus & Gyopari, 1992) and a mean lava pile thickness of  $\sim 1.5 \text{ km}$ , the total volume of lavas and sills is approximately  $2300 \text{ km}^3$ . Based on an eruption interval of  $\sim 1.6 \text{ Myr}$ , a mean eruptive rate of the Skye lavas and Little Minch Sill Complex is  $\sim 1.5 \times 10^{-3} \text{ km}^3/\text{yr}$ . This figure is consistent with a wide range of other crustal-level open magmatic systems (e.g. Crisp, 1984; White *et al.*, 2003). The volumes of the Cuillin and Redhills centres are approximately  $10^4$  and  $250 \text{ km}^3$ , respectively (based on data in Fig. 1 and Emeleus & Gyopari, 1992). Thus, the integrated mean ratio of intrusive to extrusive magma production was  $\sim 5$  in the Skye province. The mean rate of magma production (as opposed to rate of eruption) during the  $\sim 7 \text{ Myr}$  period of magmatism at Skye was  $\sim 1.7 \times 10^{-3} \text{ km}^3/\text{yr}$ . The similarity of this figure to the mean eruptive rate estimated for Skye lavas and Little Minch Sill Complex suggests that the mean rate of magma generation remained approximately constant during Skye igneous activity, although the ratio of intrusive to extrusive mass was not constant, but instead markedly increased as time progressed in the interval 61–54 Myr. Hamilton *et al.* (1998) estimated a magma production rate of  $2.2 \times 10^{-3} \text{ km}^3/\text{yr}$  for the bulk of the igneous activity at Skye based on an estimate of  $1400 \text{ km}^3$  for the combined volume of the lava succession, the mafic and ultramafic rocks of the Cuillin complex, and several high-precision Pb–U zircon dates. The agreement between our volumetric rate estimate and that of Hamilton *et al.* (1998) gives some confidence in the quality of these estimates, at least to  $\pm 20\%$ . Adopting a figure of  $2 \times 10^{-3} \text{ km}^3/\text{yr}$  implies formation of  $\sim 1.4 \times 10^4 \text{ km}^3$  of new crust over the  $\sim 7 \text{ Myr}$  interval of Skye magmatism. Averaged over the area of Skye, this corresponds to a crustal thickness increment of  $\sim 9 \text{ km}$ . The volumetric magma generation rate ( $\dot{V}$ ) of  $\sim 2 \times 10^{-3} \text{ km}^3/\text{yr}$  ( $\sim 6 \text{ Mt}/\text{yr}$ ) in the mantle beneath Skye can be used to estimate the magma heat power and ‘excess’ heat flux transferred from mantle to crust or atmosphere. The average magma heat power,  $\dot{H}$ , transferred from mantle to crust during the  $\sim 7 \text{ Myr}$  period of magmatism at Skye computed from

$$\dot{H} = \rho \dot{V} [C_p(T_m - T_a^o) + \Delta H_{\text{crystallization}}]$$

is about 0.2 GW, where  $\rho$  is magma density ( $2800 \text{ kg}/\text{m}^3$ ),  $C_p$  is the isobaric specific heat capacity ( $1200 \text{ J}/\text{kg K}$ ),  $T_m$  is the magma temperature ( $1500 \text{ K}$ ),  $T_a^o$  is the mean crustal temperature ( $800 \text{ K}$ ) and  $\Delta H_{\text{crystallization}}$  is the specific latent heat of crystallization for basalt ( $380 \text{ kJ}/\text{kg}$ ). Values for the parameters are taken from Spera (2000). Distributed uniformly over the area of the Skye igneous province ( $\sim 1650 \text{ km}^2$ ), this magma heat

power corresponds to an ‘excess’ heat flux of  $\sim 130 \text{ mW}/\text{m}^2$ . For comparison, the global mean heat flux through continental crust is currently about  $57 \text{ mW}/\text{m}^2$ . Hence, magmatism at Skye played an important, indeed dominant, role in regional geothermics and crustal growth in the Paleocene.

## Previous models

It is impossible to provide a comprehensive review of the truly voluminous literature pertaining to the geology and petrology of Skye. Here, we briefly review a few recent studies most germane to the present study. Table 1 presents an overview of the chronology, petrology and petrography of igneous rocks from the Skye Tertiary igneous centre used in this modelling study; it shows compositional ranges and textural features indicative of open-system processes and is arranged stratigraphically, from oldest at bottom, to youngest at top. The lithologic divisions of the map units shown on Fig. 1 are based on compilations from Bell (1976), Mussett *et al.* (1988), Dagley *et al.* (1990) and Hamilton *et al.* (1998). Many workers have emphasized the complex evolution of Skye magmas inferred from the lack of correlation and monotonicity between differentiation indices (such as  $\text{SiO}_2$  and  $\text{MgO}$ ), incompatible trace-element concentrations and Sr–Nd–Pb-isotope systematics. Some early studies suggested that parental magmas inherited their compositional traits from a heterogeneous Archaean subcontinental lithospheric mantle source and did not interact with the continental crust *en route* to the surface (e.g. Beckinsale *et al.*, 1978; Pankhurst & Beckinsale, 1979). More widely accepted hypotheses, however, involve variable degrees of mantle-source melting at a range of depths (Scarrow & Cox, 1995) or polybaric fractional crystallization in combination with selective crustal contamination, either by migration of elements in a fluid phase (e.g. Moorbath & Thompson, 1980; Thompson *et al.*, 1980; Dickin, 1981) or by a silicate melt composed of fusible components of Lewisian gneiss (e.g. Thompson *et al.*, 1982, 1986; Dickin *et al.*, 1987; Geldmacher *et al.*, 2002). In short, a menagerie of petrologic processes and source materials has been called upon to explain the petrogenesis of Skye Tertiary rocks.

## Nature of the crust beneath Skye

Geophysical studies indicate that the crust beneath Skye is approximately 25–28 km thick and is dominated by Archaean (Lewisian) orthogneisses (Bott & Tucson, 1973; Bamford *et al.*, 1977; Bott & Tantrigoda, 1987; Chadwick & Pharoah, 1998). Granulite-facies Lewisian gneisses (LG) form the lower crust and are overlain at mid-crustal levels by amphibolite-facies Lewisian gneisses (LA) (Weaver & Tarney, 1980, 1981). Both crustal types crop

Table 2: Range of initial (60 Ma) isotopic compositions of Lewisian granulites, amphibolites and Torridonian metasediments

	Lewisian granulites	Lewisian amphibolites	Torridonian metasediments
$^{87}\text{Sr}/^{86}\text{Sr}$	0.7020–0.7080 (0.7045–0.7063)	0.7100–0.7300 (0.7106–0.7170)	0.7171–0.7638 (0.7352)
$^{206}\text{Pb}/^{204}\text{Pb}$	13.41–19.48 (12)	13.50–19.54 (19.5)	18.61–19.23
$^{208}\text{Pb}/^{204}\text{Pb}$	33.47–38.26	35.28–44.05	37.89–39.49

Data taken from Chapman & Moorbath, 1977; Walsh *et al.*, 1979; Dickin, 1981; Thompson, 1982; Thompson *et al.*, 1982; Holden *et al.*, 1987; Whitehouse & Robertson, 1995. Values in parentheses indicate range of values used in modelling.

out on the Scottish mainland. The granulite complex is compositionally bimodal (i.e. tonalite and basic granulite), and exposed portions contain a greater proportion of mafic and ultramafic material than the amphibolite complex (Wood, 1980). The uppermost crust is made up of late Precambrian [Torridonian (T)] metasediments with ages in the range 1.1–0.75 Ga, based on a few radiometric and palaeomagnetic dates (Gass & Thorpe, 1976; Dickin & Exley, 1981). T rocks include fluvial arkosic sandstones and siltstones (Dickin & Exley, 1981) with intercalated shale beds and thin calcareous lenses present in the lower part of the succession. In the upper part, arkoses predominate. On Skye, T metasediments are overlain by a thin (~900 m) veneer of Mesozoic sediments (Gass & Thorpe, 1976).

LG, LA and T sedimentary rocks have different mean isotopic compositions and ranges (Table 2). On average, amphibolite-facies Lewisian rocks are more radiogenic (Sr and Pb) than the granulite-facies rocks (Dickin *et al.*, 1984). In comparison with Lewisian rocks, T metasediments generally have higher  $^{87}\text{Sr}/^{86}\text{Sr}$  and  $^{206}\text{Pb}/^{204}\text{Pb}$ . The range of  $^{208}\text{Pb}/^{204}\text{Pb}$  for T sediments lies within the range of Lewisian amphibolite (LA) gneiss (Dickin & Exley, 1981; Dickin *et al.*, 1984). These relations are summarized in Table 2.

## EC-RAFC GEOCHEMICAL TRAJECTORIES

In the section below, we apply the EC-RAFC simulator in order to quantify petrogenetic processes relevant to the Skye Tertiary igneous rocks. We have broken the complex ~7 Myr magmatic history of Skye into three main lithologic lineages (L1, L2 and L3). The lineages are defined based on geologic criteria, including spatial relatedness, petrologic affinity and radiometric and palaeomagnetic geochronology deduced from previous workers (Thompson, 1969; Thompson *et al.*, 1972; Dickin, 1981; Dickin & Exley, 1981; Bell, 1983; Bell & Harris, 1986; Tantrigoda, 1988; Dagley *et al.*, 1990; Gibson, 1990; Emeleus & Gyopari, 1992; Scarrow, 1992; Bell *et al.*,

1994; Hamilton *et al.*, 1998), as summarized in Table 1. These lineages provide the framework for the computation of EC-RAFC geochemical trajectories. Additional lineages may be present, but are not considered here because of lack of geochemical data. Table 3 provides the salient features of the defined lineages, including cross-reference to the lithologic units summarized in Table 1, the approximate range of observed silica contents, Pb- and Sr-isotope ratios, Sr abundance, likely crustal contaminants (see Table 2) and the name of each EC-RAFC trajectory. There are three EC-RAFC trajectories for lineage L3 (EC3A, EC3B and EC3C), two for lineage L2 (EC2A and EC2B) and five for lineage L1 (EC1A, EC1B, EC1C, EC1D and EC1E). Hence, 10 distinct EC trajectories were used to model the ~7 Myr magmatic evolution at Skye. Sr- and Pb-isotope data and Sr-concentration data used to gauge the quality of the EC models are shown in Fig. 2a–d. In that figure and on computed EC-RAFC trajectories, the raw data are plotted (broken into L1, L2 or L3) to facilitate comparison between observation and model.

The EC-RAFC model provides information on any trace-element and isotope ratio of interest. Unfortunately, the trace-element and isotope geochemistry database on Skye rocks relevant to L1, L2 and L3 is incomplete. Compared with other geochemical data, abundant published Sr-isotope data do exist for a wide range of Skye Tertiary igneous rocks and, consequently, we have focused upon  $^{87}\text{Sr}/^{86}\text{Sr}$ , Sr abundance and (to a lesser extent) Pb-isotopes in the modelling efforts. The available Nd-isotopic dataset (e.g. Dickin *et al.*, 1984, 1987; Gibson, 1990; Scarrow, 1992; Ellam & Stuart, 2000) is insufficient for our purposes. However, as a wider range of geochemical measurements on single unaltered samples become available, the validity of the EC-RAFC ‘solutions’ developed in this study can be explicitly and easily tested. A great value of the EC-RAFC model is that it leads to quantitative predictions for relative masses and compositions of derivative melts, cumulate rocks, enclaves and preserved mixed magmas in a relative temporal sequence.

Table 3: The Skye Tertiary igneous centre: lineages and EC modelling trajectories

Magmatic lineage	Lithologic unit	SiO <sub>2</sub> range	<sup>87</sup> Sr/ <sup>86</sup> Sr range	<sup>206</sup> Pb/ <sup>204</sup> Pb range	[Sr]	Crustal contaminant	EC-RAFC trajectory
1	SMLS Fe-poor lavas	46–54	0.703 06–0.704 72		619–809	LG	EC1A
	SMLS Fe-poor lavas, Outer Unlayered Gabbro (C1), northern C2 intrusions, C3 granites	58–78	0.704 89–0.710 65		9–387	LA	EC1B
	SMLS Fe-poor lavas, southern C2 gabbro & granite intrusions, C3 mafic sill	50–71	0.705 07–0.712 77		102–344	LA	EC1C
	C3 granites	70–72	0.710 68–0.716 06		62–140	LA	EC1D
	C3 granites	70–74	0.710 68–0.713 74		80–140	LA	EC1E
2	PMB lavas, C1 mafic intrusions	46–49	0.703 00–0.703 45		102–240	LA	EC2A
	C1 mafic intrusions, Coire Uaigneich Granophyre (C1)	~49–75	0.710 72–0.733 19		86–148	T	EC2B
3	SMLS Fe-rich lavas	45–46	0.703 08–0.704 03	17.41–15.63	353–658	LG	EC3A
	SMLS Fe-rich lavas & Little Minch Sill Complex	47–49	0.704 05–0.704 80	15.78–15.35	250–583	LG	EC3B
	SMLS Fe-rich lavas & Little Minch Sill Complex	47–50	0.704 83–0.705 31	15.84–17.61	260–366	LA	EC3C

Data sources are cited in Table 1 and Figs 3–5. SiO<sub>2</sub> ranges are approximate—SiO<sub>2</sub> data are not available for some samples included in EC-RAFC modelling and data from igneous bodies not included in modelling have been reported where appropriate.

### Definition of petrologic lineages

Criteria used to define the lineages are discussed in detail in this section. The bulk of the Skye lava field is made up of light rare earth element (LREE)-enriched transitional alkali basalts and less abundant hawaiites–trachytes of the SMLS (Thompson *et al.*, 1972, 1982; Scarrow, 1992). SMLS MgO contents can be as low as ~1 wt % and as high as ~14 wt %. Most of the SMLS magnesian (>9 wt % MgO) lavas do not have geochemical features traditionally associated with primary magmas; the lavas often display unradiogenic Pb- and radiogenic Sr-isotope compositions similar to those of the underlying Archaean Lewisian gneisses (Scarrow, 1992). Thompson *et al.* (1972) showed that within the SMLS, there are products of two contrasting differentiation series: Fe-rich basalts–benmoreites exposed in northern and central Skye and Fe-poor intermediate compositions, which have been sampled mainly in central Skye.

In our classification scheme, lineage L1 (Table 3) consists of SMLS low-Fe intermediate-type Skye lavas that mainly occur in the upper portion of the lava field (Dickin *et al.*, 1984). Based on major and trace-element and Pb-isotopic similarity to SMLS-type lavas (Dickin *et al.*, 1984), the earliest intrusion of the Cuillin centre (the Outer Unlayered Gabbro; Table 1) and all Western and Eastern Redhills intrusions (Table 1) are also included in L1.

Lineage L2 (Table 3) rocks include PMB-type Skye lavas from the uppermost part of the lava pile, as well as all intrusions of the Cuillin centre except the Outer

Unlayered Gabbro (Table 1). PMB flows are MORB-like, LREE-depleted, high-calcium, alkali-poor olivine tholeiites. These are intercalated with SMLS-type flows at the top of the Skye lava field in west-central Skye. SMLS and PMB lavas are distinct on element–element, element–isotope and isotope–isotope plots such as [Sr] versus <sup>87</sup>Sr/<sup>86</sup>Sr and <sup>206</sup>Pb/<sup>204</sup>Pb versus <sup>208</sup>Pb/<sup>204</sup>Pb (Fig. 2a and d). Unlayered Cuillin intrusions have major element abundances similar to the PMB-type lavas and the Cuillin complex has been interpreted as coeval with the PMB lavas (Thompson *et al.*, 1972; Thompson, 1982; Scarrow, 1992; Stuart *et al.*, 2000). The PMB flows are believed to represent the remnants of an originally significant lava shield that developed above the Cuillin centre (Williamson & Bell, 1994).

Lineage L3 (Table 3) comprises SMLS Fe-rich lavas that are mainly *ne* normative at low <sup>87</sup>Sr/<sup>86</sup>Sr. These form most of the lowermost flows and are volumetrically dominant in the Skye lava field (Table 1). On the basis of compositional and spatial affinities (Gibson, 1990), the sills of the Little Minch Sill Complex (Table 1) are categorized in lineage L3. Little Minch Sill Complex sills intrude Jurassic sediments in northern Skye and on nearby islands (Fig. 1) (Gibb & Gibson, 1989). Intrusive relationships indicate that the Little Minch Sill Complex is marginally younger than the majority of SMLS lavas (Gibson, 1988). Olivine cumulate-rich picrite, picrodolerite and alkali dolerite are the main lithologies (Gibb & Gibson, 1989). The sills can be mono- or polylithologic and the presence of internal chills at lithologic boundaries

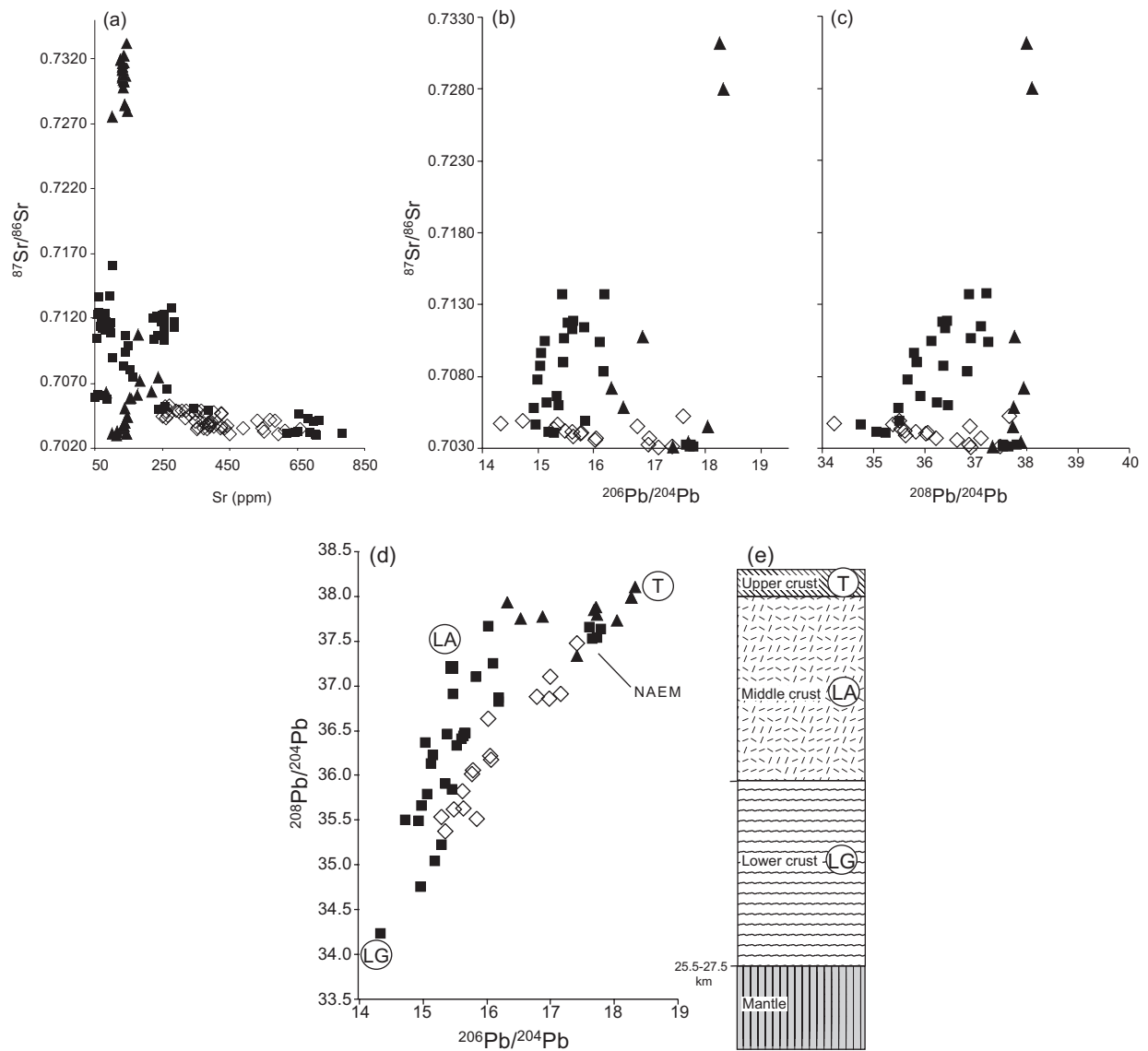


**Fig. 2.** (a) Plot of [Sr] ppm versus initial  $^{87}\text{Sr}/^{86}\text{Sr}$  data for the Skye samples included in the present study (Moorbath & Bell, 1965; Carter *et al.*, 1978; Dickin & Exley, 1980; Dickin *et al.*, 1980, 1984; Moorbath & Thompson, 1980; Dickin, 1981, 1983; Thompson *et al.*, 1982, 1986; Gibson & Jones, 1991; Scarrow, 1992; Bell & Pankhurst, 1993; Bell *et al.*, 1994; Ellam & Stuart, 2000). (b)–(d) Plots of initial  $^{206}\text{Pb}/^{204}\text{Pb}$ – $^{87}\text{Sr}/^{86}\text{Sr}$ ,  $^{208}\text{Pb}/^{204}\text{Pb}$ – $^{87}\text{Sr}/^{86}\text{Sr}$  and  $^{206}\text{Pb}/^{204}\text{Pb}$ – $^{208}\text{Pb}/^{204}\text{Pb}$  data for the Skye samples included in the present study (Moorbath & Welke, 1969; Dickin, 1981; Dickin & Exley, 1981; Dickin *et al.*, 1984; Stuart *et al.*, 2000).  $^{206}\text{Pb}/^{204}\text{Pb}$ – $^{208}\text{Pb}/^{204}\text{Pb}$  for crustal lithologies are indicated (Dickin, 1981). LG, granulite-facies Lewisian gneiss; LA, amphibolite-facies Lewisian gneiss; T, Torridonian metasediments. NAEM is the North Atlantic End Member (Ellam & Stuart, 2000). (e) Potential crustal contaminants beneath Skye, LG (rippled lines), LA (crosshatch) and T. The thickness of the crust is taken from Chadwick *et al.* (1998). In Fig. 2 and following figures: squares, L1 data; triangles, L2 data; diamonds, L3 data.

and within lithologic units suggests that multiple intrusions occurred. The picrodolerite unit, which exhibits element and isotope signatures similar to SMLS lavas, is considered in this study. The crininite and picrite units are chemically and texturally distinct (Gibson & Jones, 1991). These units are not examined here because of a lack of relevant chemical data.

The assumption that SMLS- and PMB-type magmas have distinct parental liquids is supported by gravity data

showing that both the Red Hills and Cuillin centres of the Skye central complex are associated with distinct, strong, positive Bouguer gravity anomalies. These are attributed to the presence of a large mass of mafic to ultramafic rock, extending to depths of at least 15 km beneath the central complex (Bott & Tucson, 1973). In addition, results from palaeomagnetic investigations show that the L2 rocks are reversely magnetized, whereas the L1 rocks have normal polarities. Therefore, there must

have been at least two periods when mafic magmas were introduced into the Skye centre; those for L2 were intruded when the Earth's magnetic field polarity was reversed, and those of L1 when the field was normal. No exposed record of intrusions associated with the L3 lavas is preserved.

### Alteration

Petrographic, isotopic and mineralogical investigations (e.g. Bailey *et al.*, 1924; Tilley & Muir, 1962; Taylor & Forrester, 1971; Forrester & Taylor, 1977; Ferry, 1985) showed that BTIP rocks have interacted widely with heated groundwater. This led to the suggestion that Pb- and Sr-isotope compositions in BTIP rocks may have undergone significant post-solidification alteration. All subsequent geochemical work has had to take this problem into account.

Several studies have concluded that alteration is minimal in carefully selected samples (Thompson *et al.*, 1972; Hawkesworth & Morrison, 1978; Dickin *et al.*, 1980; Moorbath & Thompson, 1980; Scarrow & Cox, 1995). For example, Dickin *et al.* (1980) showed that significant isotopic disturbance in the Coire Uaigneich Granophyre is found only within 1.5 cm of major fractures. Skye lavas typically have amygdaloidal upper and lower layers, and massive central portions (Scarrow & Cox, 1995). Hawkesworth & Morrison (1978) measured vertical Sr-isotope variation in a BTIP lava flow from a greenschist-facies zone of hydrothermal alteration on Mull and found that the whole-rock  $^{87}\text{Sr}/^{86}\text{Sr}$  isotope composition of the flow centre was the same as that of separated fresh pyroxene. They concluded that the flow centre was essentially unaffected by hydrothermal alteration. Subsequent workers have minimized the effects of alteration on the Skye geochemical dataset by collecting samples from the interior parts of intrusions and lava flows. Data used to assess the quality of the EC-RAFC trajectories in this study are restricted to those interpreted as being minimally altered by previous workers.

### EC-RAFC model: overview

EC-RAFC tracks the trace-element and isotopic composition of melt, cumulates, country-rock partial melts and enclaves during simultaneous recharge, assimilation and fractional crystallization. EC-RAFC is formulated as an initial value problem based on a set of  $3 + t + i + s$  coupled differential equations, where the number of trace elements, radiogenic and stable-isotope ratios simultaneously and self-consistently modelled are  $t$ ,  $i$  and  $s$ , respectively. Solution of the EC-RAFC equations provides values for the average wall-rock temperature ( $T_a$ ), mass of melt within the

magma body ( $M_m$ ), mass of cumulates ( $M_c$ ) and enclaves ( $M_{en}$ ), mass of wall rock involved in the thermal interaction ( $M_a^o$ ), mass of anatectic melt assimilated ( $M_a^*$ ), and concentration of  $t$  trace elements and  $i + s$  isotopic ratios in melt ( $C_m$ ), cumulates ( $C_c$ ), enclaves ( $C_{en}$ ), and anatectic melt ( $C_a$ ) as a function of magma temperature ( $T_m$ ). Input parameters include the equilibration temperature ( $T_{eq}$ ), the initial temperature and composition of pristine melt ( $T_m^o$ ,  $C_m^o$ ,  $\epsilon_m^o$ ), recharge melt ( $T_r^o$ ,  $C_r^o$ ,  $\epsilon_r^o$ ) and wall rock ( $T_a^o$ ,  $C_a^o$ ,  $\epsilon_a^o$ ), temperature-dependent trace-element distribution coefficients ( $D_m$ ,  $D_r$ ,  $D_a$ ), heats of transition for wall rock ( $\Delta h_a$ ), pristine melt ( $\Delta h_m$ ) and recharge melt ( $\Delta h_r$ ), and the isobaric specific heat capacity of assimilant ( $C_{p,a}$ ), pristine melt ( $C_{p,m}$ ) and recharge melt ( $C_{p,r}$ ). The magma recharge mass function,  $M_r(T_m)$  is specified *a priori* and defines how recharge magma is added to standing magma. In addition to detailed geochemical information generated in a complete EC-RAFC trajectory, a few specific measures are especially useful. These include  $M_a^*/M_a^o$ , an indication of the extent of partial melting in the country rock surrounding the magma body,  $\lambda \equiv \chi M_a^*/M_a^o$ , a measure of the extent of magma contamination,  $\Sigma M_r$ , the sum of all increments of recharge, and  $M_c$ , the mass of cumulates formed by fractional crystallization. Details of the EC models have been described by Spera & Bohrson (2001, 2002, 2004) and Bohrson & Spera (2001, 2003). In this work, the parameter  $\chi$  is set to unity.

The models were run iteratively to maximize agreement between model and observed data, while maintaining geologically reasonable values for input parameters. Geochemical data for assimilants (T, LA and LG) and for liquid (melt) compositions are taken from the literature sources cited above and are summarized in Tables 1–3. Laboratory studies (see, e.g. Bergantz & Dawes, 1994; Petford & Gallagher, 2001; Spera and Bohrson, 2002, for a summary) constrain melt productivity functions [ $f_a(T_a)$ ,  $f_m(T_m)$  and  $f_r(T_r)$ ] for the end-member compositions used in EC-RAFC models. Melt-productivity curves exhibit non-linear sigmoid forms in melt fraction versus temperature coordinates at fixed pressure and volatile species fugacity (e.g.  $f_{O_2}$ ,  $f_{H_2O}$ ,  $f_{CO_2}$ ). Multicomponent equilibrium thermodynamic calculations (e.g. MELTS, Ghiorso, 1995) similarly exhibit sigmoidal melt-productivity curves. The melt-production curves used in this study are based on both experiments and MELTS calculations for appropriate compositions based on protoliths in Table 2 and magma bulk compositions. Phase transition enthalpies and specific heats are taken from compilations by Spera (2000) and Spera & Bohrson (2001). The temperature dependence of trace-element partition coefficients yields a range of distribution coefficients for a particular temperature range and are taken from the literature or estimated.

### *Choice of Sr–Pb-isotope composition of parental magma*

Each lineage corresponds to an evolutionary trend starting from a well-defined and distinct parental liquid. Here, we describe the rationale for selection of Pb- and Sr-isotope initial values. The unradiogenic  $^{206}\text{Pb}/^{204}\text{Pb}$  and  $^{208}\text{Pb}/^{204}\text{Pb}$  signatures of many of the earliest-erupted Skye Tertiary rocks (SMLS) have long been proposed as evidence of interaction with Lewisian granulite (LG)-facies crust (e.g. Moorbath & Welke, 1969; Dickin, 1981; Dickin *et al.*, 1984). The PMB lavas form a separate trend that extends towards Pb-isotopic values similar to LA gneiss (Fig. 2d). Those Skye lavas with the most radiogenic Pb are of similar composition to the North Atlantic End Member (NAEM)—a hypothetical uncontaminated mantle-derived melt composition proposed by Ellam & Stuart (2000), which is defined by the convergence of Pb-isotope trends of rocks from numerous localities within the BTIP and elsewhere in the North Atlantic Igneous Province (Fig. 2d). According to Ellam & Stuart (2000), Pb-isotope variations in rocks from different locations within the BTIP indicate local variation in the nature of crustal contaminants. We identified as parental compositions NAEM-like Skye lavas. These are present within each lineage and generally have the lowest  $^{87}\text{Sr}/^{86}\text{Sr}$  values (0.703 00–0.703 08). An assessment of the changes in Sr-isotopes up-section, coupled with covariations in MgO- and Pb-isotopes, suggest that recharge and assimilation add radiogenic Sr.

### **EC-RAFC modelling: results and petrogenetic implications**

Each of the three petrologic lineages is further divided into sublineages for the purpose of comparing observations (geochemical data) with EC-RAFC modelling trajectories. It is important to note that within a given lineage, the sublineages form an evolutionary sequence such that the letter 'A' denotes the first sublineage and subsequent sublineages are denoted alphabetically. Within a lineage, successive model input parameters follow from the previous model. For example, the input for model EC1B is the final state of model EC1A. We distinguish data from EC-RAFC models by using, for example, the label L1A to refer to a sublineage of rocks and the symbol EC1A to refer to a computed EC-RAFC geochemical trajectory.

#### *Lineage 1: sublineages, model results and petrogenetic implications*

*L1: sublineages.* For the purpose of modelling, L1 data are subdivided into five sublineages based on spatial and compositional characteristics. Each sublineage is modelled as a separate EC-RAFC trajectory, labelled EC1A, EC1B, EC1C, EC1D, and ECE on the diagrams that follow. L1A consists of Skye lavas of SMLS low-Fe intermediate type. The lavas are hawaiites, mugearites

and benmoreites that contain plagioclase and magnetite phenocrysts as well as sparse-to-absent olivine phenocrysts (Thompson *et al.*, 1972). The L1A data form a negative  $^{206}\text{Pb}/^{204}\text{Pb}$ – $^{87}\text{Sr}/^{86}\text{Sr}$  trend. The most evolved L1A samples have  $^{87}\text{Sr}/^{86}\text{Sr}$  similar to the least radiogenic L1B samples (Fig. 3).

At the lowest  $^{87}\text{Sr}/^{86}\text{Sr}$  values, L1B includes samples from the upper part of the Skye lava field (Table 1) and the Outer Unlayered Gabbro (OUG) of the Cuillin centre (Table 1); other samples are from intrusions in the northern part of the Western Redhills centre (Table 1) and the Outer Granite (Table 1) of the Eastern Redhills centre (Fig. 3). Samples in L1C come from intrusions exposed in the southern part of the Western Redhills centre (Table 1), from the basaltic andesite facies of the Rubha'an Eireannaich mafic–silicic composite sill (Table 1), and the Outer Granite (Table 1) of the Eastern Redhills centre (Fig. 3). There is field evidence that the Western Redhills intrusions may have distinct petrogenetic histories. Intrusions in the southern part of the Western Redhills centre are separated from a group of intrusions in the northern part of the centre by a mass of vent agglomerates, crushed gabbro and basaltic lavas (Emeleus & Gyopari, 1992). Table 1 summarizes the igneous chronology at the northern and southern parts of the centre, respectively. Sr-isotopic values within L1B and L1C increase progressively with increasing stratigraphic height, according to the sequence outlined in Table 1. The L1B and L1C samples display a broad positive  $^{206}\text{Pb}/^{204}\text{Pb}$ – $^{87}\text{Sr}/^{86}\text{Sr}$  correlation.

The Western Redhills centre is renowned for preserving hybrid rocks that display a wide range of magma-mixing phenomena (Wager *et al.*, 1965; Thompson, 1980; Vogel *et al.*, 1984). The presence of mafic inclusions in some granitic intrusions (e.g. the Glamaig Granite and Northern Porphyritic Granite; Table 1), as well as the hybrid nature of the Marscoite and Marscoite–Glamaigite mixed suites (Table 1), indicate that recharge was important in the magmatic evolution of L1B and L1C magmas. Remnants of Tertiary basalt on top of some granites show that the granitic magmas intruded into high levels in the crust (Gass & Thorpe, 1976).

All samples in L1D and L1E are from either the Outer Granite (Table 1) or the rhyolite–intermediate facies of the Rubha'an Eireannaich sill (Table 1) of the Eastern Redhills centre. The Rubha'an Eireannaich sill is one of a suite of mafic–silicic composite sills (Harker, 1904; Bell & Pankhurst, 1993) in which boundaries between marginal basaltic andesite and a central rhyolite portion are gradation in terms of mineralogy and texture (Bell & Pankhurst, 1993). There are no internal contacts. Bell & Pankhurst (1993) performed serial sampling across the sill and observed that compositional profiles for major and trace elements and Sr-isotopes exhibit continuous

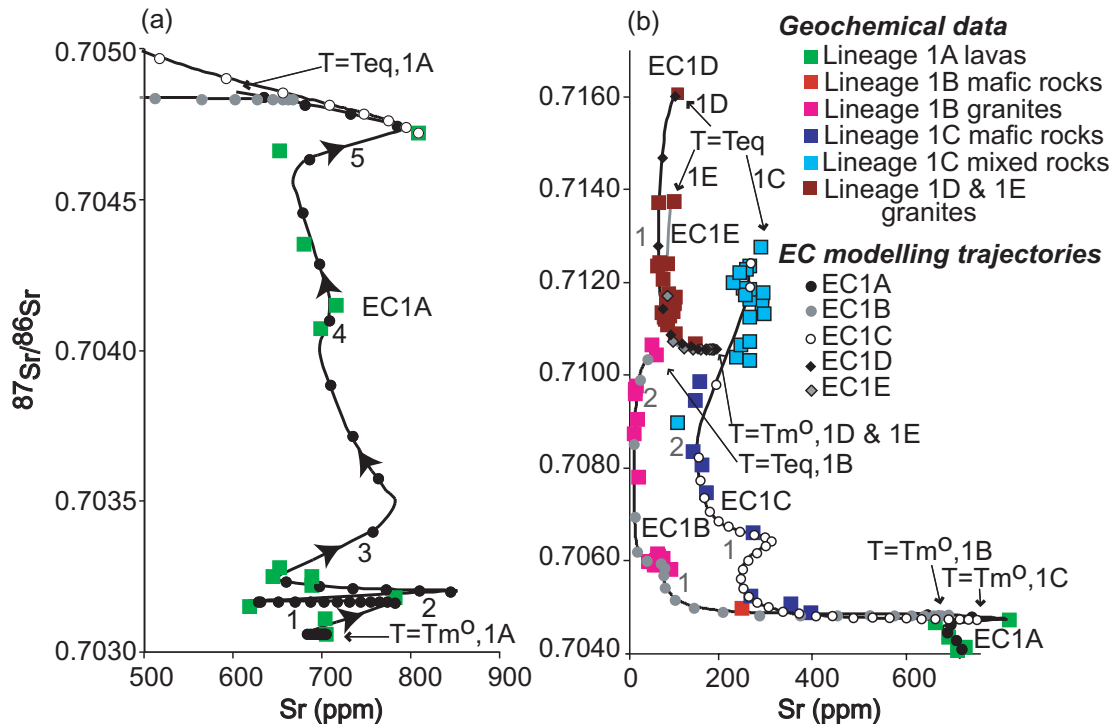


**Fig. 3.** (a) Plot of [Sr] ppm versus initial  $^{87}\text{Sr}/^{86}\text{Sr}$  data (SMLS lavas; see Fig. 2 for data references) and results of EC-RAFC simulations (EC1A) for lineage L1A. Temperature drop for each symbol of the EC-RAFC trend:  $4\text{--}7^\circ\text{C}$ . (b) [Sr] versus  $^{87}\text{Sr}/^{86}\text{Sr}$  data (SMLS lavas, Western and Eastern Redhills intrusions, Outer Layered Gabbro of Cuillin centre; see Fig. 2 for data references) and results of EC-RAFC simulations (EC1B, EC1C, EC1D and EC1E) for lineages L1B, L1C, L1D and L1E. Temperature drop for each symbol of the EC-RAFC trends:  $8\text{--}39^\circ\text{C}$  (EC1B),  $17\text{--}4^\circ\text{C}$  (EC1C),  $5\text{--}5^\circ\text{C}$  (EC1D and EC1E). Arrows represent direction of falling magma temperature. Numbers on EC-RAFC trends show recharge episodes. Table 4 shows mass and temperature of recharge magma increments.

gradients. The Outer Granite is a group of intrusions that is peripheral to a second group of intrusions, the Inner Granite (Bell & Harris, 1986). Because of a scarcity of Sr-isotope, major- and trace-element data, the Inner Granite is not considered in this study.

**L1: model results.** Input parameters for all EC1 simulations are shown in Table 4. In the EC1A model, the parental sample has an initial Sr-isotope value of 0.70315 and 4.26 wt % MgO. The modelled country-rock Sr-isotope ratio and Sr-concentration parameters are similar to published values for leucocratic to mesocratic LG-facies gneiss (Weaver & Tarney, 1980; Dickin, 1981). Invoking LG as the contaminant is consistent with the negative correlation between  $^{206}\text{Pb}/^{204}\text{Pb}$  and  $^{87}\text{Sr}/^{86}\text{Sr}$  and also with thermal parameters that suggest the magma chamber resided within the lower crust. For consistency with the presence of plagioclase (e.g. Thompson *et al.*, 1972), Sr is modelled as compatible in the host magma and incompatible in the country rock in EC1A and all other EC-RAFC simulations for lineage L1 data. MELTS (Ghiorso, 1997) liquidus temperature simulations based on the major-element chemistry of the parental sample yield a magma liquidus temperature close to  $1302^\circ\text{C}$  at

1 GPa (a pressure equivalent to lower-crustal depths) (Thompson *et al.*, 1972).

The  $^{87}\text{Sr}/^{86}\text{Sr}$  value of the recharge magma is higher than that of the uncontaminated host magma in EC1A and all other EC1 models. In EC1A, five episodes of magma recharge are modelled to coincide with sharp observed increases in Sr concentrations or deviations in  $^{206}\text{Pb}/^{204}\text{Pb}$  towards higher values. Sr is incompatible in the recharge magma. Table 4 shows the temperatures and normalized masses at which recharge magma mixes with host magma.

Table 4 shows  $M_a^*$ , the mass of anatectic melt assimilated into the magma,  $M_c$ , the mass of cumulates in the magma body, and  $M_a^o$ , the mass of country rock involved in the EC-RAFC event, for EC1A and all other EC1 models. The mass of recharge magma,  $M_r^o$ , is specified *a priori*. In the EC-RAFC simulations discussed in the present study, all melt generated in the country rock is assimilated into the magma body (i.e.  $\chi = 1$ ). The ratio of the mass of anatectic melt to the mass of cumulates in EC1A ( $M_a^*/M_c = 3.81$ ) is higher than in other EC1 models. The input of relatively large masses of recharge magma ( $\sum M_r^o = 5.22$ ) early in the EC1A RAFC episode limits the effect of fractional crystallization. As a

Table 4: EC-RAFC parameters, Lineage 1

<i>Thermal parameters</i>	EC1A	EC1B	EC1C	EC1D	EC1E
Magma liquidus temperature, $T_{l,m}$	1300°C	1111°C	1125°C	830°C	830°C
Magma initial temperature, $T_m^o$	1300°C	1111°C	1125°C	830°C	830°C
Assimilant liquidus temperature, $T_{l,a}$	1222°C	980°C	1100°C	1000°C	1000°C
Assimilant initial temperature, $T_a^o$	660°C	200°C	220°C	450°C	550°C
Recharge magma liquidus temperature, $T_{l,r}$	1340°C	1090°C	1100°C	1040°C	1040°C
Recharge magma initial temperature, $T_r^o$	1340°C	1090°C	1100°C	1040°C	1040°C
Solidus temperature, $T_s$	940°C	715°C	735°C	715°C	715°C
Equilibration temperature, $T_{eq}$	1105°C	717°C	739°C	765°C	777°C
Crystallization enthalpy, $\Delta h_m$ (J/kg)	396000	396000	350000	380000	380000
Isobaric specific heat of magma, $C_{p,m}$ (J/kg K)	1495	1470	1372	1450	1450
Fusion enthalpy, $\Delta h_a$ (J/kg)	370000	395000	420000	395000	395000
Isobaric specific heat of assimilant, $C_{p,a}$ (J/kg K)	1400	1500	1450	1500	1500
Crystallization enthalpy of recharge magma, $\Delta h_r$ (J/kg)	410000	370000	350000	350000	350000
Isobaric specific heat of recharge magma, $C_{p,r}$ (J/kg K)	1500	1470	1372	1450	1450
<i>Mass and temperature of recharge magma</i>					
Recharge episode 1	1-40, 1250°C	0-56, 830°C	0-65, 840°C	0-85, 805°C	—
Recharge episode 2	2-00, 1190°C	0-02, 754°C	0-15, 755°C		
Recharge episode 3	0-71, 1159°C				
Recharge episode 4	0-07, 1140°C				
Recharge episode 5	1-04, 1124°C				
<i>Compositional parameters</i>					
	Sr	Sr	Sr	Sr	Sr
Magma initial concentration (ppm), $C_m^o$	705	667	809	180	180
Magma isotope ratio, $\epsilon_m^o$	0-70306	0-70483	0-70472	0-71055	0-71055
Magma trace-element distribution coefficient, $D_m$ , and range	1-26 1-85–1-95	0-36 1-96–3-85	1-30 1-68–1-86	1-08 2-32–2-43	2-35
Enthalpy of trace-element distribution reaction, $\Delta H_m$	–5000	–19500	–3000	–7000	—
Assimilant initial concentration (ppm), $C_a^o$	427	400	275	540	250
Assimilant isotope ratio, $\epsilon_a^o$	0-70626	0-71060	0-71550	0-71700	0-71700
Assimilant trace-element distribution coefficient, $D_a$ , and range	0-07 0-50–0-27	0-85	0-75	0-80 0-35–0-45	0-24
Enthalpy of trace-element distribution reaction, $\Delta H_a$	–15000	—	—	5000	—
Recharge magma initial concentration (ppm), $C_r^o$	765	800	600	230	230
Recharge magma isotope ratio, $\epsilon_r^o$	0-70322	0-70600	0-70670	0-71200	0-71200
Recharge magma trace-element distribution coefficient, $D_m$ , and range	0-05	0-09 0-73–1-66	0-74	1-80	1-80
Enthalpy of trace-element distribution reaction, $\Delta H_r$	—	–24000	—	—	—
<i>Mass characteristics</i>					
Mass of assimilant partial melt, $M_a^*$	3-01	0-01	0-02	0-04	0-03
Mass of cumulates, $M_c$	0-79	0-99	0-99	0-84	0-63
Mass of recharge magma, $M_r^o$	5-22	0-58	0-80	0-85	0
Mass of country rock involved in RAFC event, $M_a^o$	5-0	1-9	2-0	2-2	0-9

result of the large proportion of recharge magma involved in EC1A, the proportion of anatectic melt that is incorporated ( $\lambda = M_a^*/M_a^o = 0.60$ ) is greater than in other L1 EC-RAFC models.

Figure 3 shows EC1A, the computed EC-RAFC trajectory for L1A  $[Sr]^{-87}Sr/^{86}Sr$  data. The addition of two pulses of recharge magma ('1' and '2', Fig. 3a) during the heating of country rock from its initial temperature to the solidus causes  $^{87}Sr/^{86}Sr$  to become slightly more radiogenic. Because Sr is incompatible in the recharge magma,  $[Sr]$  of the host magma increases during these recharge episodes. When assimilation begins,  $^{87}Sr/^{86}Sr$  in the magma increases significantly because of the incorporation of more radiogenic assimilate. During intervals in which the evolution of the magma body is dominated only by assimilation and fractional crystallization processes,  $[Sr]$  of the magma body decreases because of the strong compatibility of Sr in the magma and the relatively low  $[Sr]$  of incoming anatectic melt. When recharge magma is mixed into host magma,  $[Sr]$  increases.

Thermal and geochemical input parameters in the EC1B model corresponds to the most radiogenic  $^{87}Sr/^{86}Sr$  samples of EC1A and EC1C input parameters correspond to the most radiogenic  $^{87}Sr/^{86}Sr$  samples of EC1B (Fig. 3b). In contrast to the L1A data, the positive correlation between L1B and L1C  $^{87}Sr/^{86}Sr$  and radiogenic Pb-isotopic values suggests that L1B and L1C magmas are contaminated with LA gneiss. The presence of LA xenoliths in L1B and L1C rocks (Thompson, 1969, 1981) supports this hypothesis. Country-rock Sr-isotope values in the EC1B and EC1C models are therefore similar to those of LA-facies gneiss and are consistent with thermal parameters reflecting middle- to upper-crustal conditions (e.g. Holden *et al.*, 1987; Whitehouse, 1990). In the EC1B model, the range of the country-rock distribution coefficient reflects varying plagioclase contents in the country rock as observed in LA xenoliths (Thompson, 1980, 1981). The compatibility of Sr in the EC1B host magma is modelled to increase to accommodate observed changes in plagioclase abundance (e.g. Thompson, 1969; Vogel *et al.*, 1984).

In the EC1B and EC1C models, the country-rock initial temperature is typical of upper-crustal conditions. Thompson (1981) performed melting experiments on LA xenoliths from L1B rocks at 1 bar pressure and observed a solidus temperature of 715°C for leucocratic and mesocratic compositions. At 952°C, the mesocratic compositions were more than 80% liquid, with several percent residual orthopyroxene and plagioclase. The modelled EC1B solidus and country-rock liquidus temperatures reflect these results. Experimentally determined solidus temperatures for L1C and L1B intrusions (Thompson, 1983; Ferry, 1985) provide approximate limits on the equilibration temperatures of L1B and L1C magmas.

The selection of Sr-concentration, Sr-isotope and distribution coefficient parameters for the recharge magma is based on the assumption that the EC1B recharge magma is similar to that which injected the EC1A magma reservoir. Plagioclase is hypothesized to join the recharge magma liquidus (i.e. the melt was multiply saturated, perhaps by cotectic crystallization) during the EC1B RAFC event, and Sr is modelled as compatible in the recharge magma in the EC1C simulation.

Of note in EC1B is the flat  $[Sr]^{-87}Sr/^{86}Sr$  trajectory at the lowest  $^{87}Sr/^{86}Sr$  values. This indicates that this part of the differentiation history is dominated by fractional crystallization. This suggests that the country rock had a relatively low initial temperature. As a consequence, the relative mass of assimilate incorporated into the host magma body is small, with  $\lambda = M_a^*/M_a^o = 0.005$ .

During the first addition of recharge magma in EC1B,  $^{87}Sr/^{86}Sr$  increases, but although  $[Sr]$  in the recharge magma is relatively high, the first episode of recharge does not lead to an increase in  $[Sr]$  in the host magma. This is because the Sr-distribution coefficient in the host magma is high as a result of melt saturation with plagioclase-bearing cumulates. When the second pulse of magma recharge takes place,  $[Sr]$  in the host magma is lower and there is a minor increase in host magma  $[Sr]$ .

The form of EC1C is broadly similar to that of EC1B (Fig. 3). However, the greater mass of recharge magma involved in EC1C ( $M_r^o = 0.80$ ) compared with EC1B ( $M_r^o = 0.58$ ), as well as the incompatibility of Sr in the recharge magma throughout EC1C, leads to greater increases in  $[Sr]$  during the addition of recharge magma. The fraction of assimilated crust in EC1C ( $M_a^* = 0.02$ ) and the proportion of assimilate ( $\lambda = M_a^*/M_a^o = 0.012$ ) are similar to those of EC1B ( $M_a^* = 0.01$ ;  $\lambda = M_a^*/M_a^o = 0.005$ ).

In  $Sr^{-87}Sr/^{86}Sr$  coordinates (Fig. 3b), data from the Outer Granite form multiple trajectories, which may reflect complex magma dynamics associated with the formation of silicic compositions or the effects of alteration (Ferry, 1985). For illustrative purposes, we have modelled only two trends, EC1D and EC1E. In the Rubha'an Eireannaich sill, the lowest initial  $^{87}Sr/^{86}Sr$  values (0.70749–0.70990) are present in the ferrobasic andesite facies, which is chemically similar to L1C intrusions of the Western Redhills centre. The highest  $^{87}Sr/^{86}Sr$  values (0.71244–0.71248) are in samples from the central rhyolite facies. These samples are chemically similar to Eastern Redhills intrusions. Samples of intermediate composition have intermediate initial  $^{87}Sr/^{86}Sr$  values (0.71069–0.71092).

Initial magma model parameters for EC1D and EC1E are broadly similar to more radiogenic  $^{87}Sr/^{86}Sr$  samples in EC1C and country-rock geochemical parameters are similar to published values for LA (e.g. Dickin, 1981). Although the model requires a higher country-rock initial

temperature for EC1E than for EC1D, in general, these initial temperatures reflect middle- to upper-crustal conditions, which, in these cases, leads to insignificant proportions of assimilant being incorporated into the EC1D and EC1E magma bodies. Despite this, the contaminated magmas have relatively high  $^{87}\text{Sr}/^{86}\text{Sr}$  because the assimilant has a high Sr-isotope ratio. The EC1D model involves a larger mass of country rock ( $M_a^o = 2.2$ ) and a smaller ratio of assimilated melt to mass of cumulates removed ( $M_a^*/M_c = 0.048$ ) than EC1E ( $M_a^o = 0.9$ ;  $M_a^*/M_c = 0.476$ ).

*L1: petrogenetic implications of EC-RAFC results.* EC-RAFC modelling results indicate that L1 magmas initially resided in a lower-crustal reservoir. We speculate that the repeated input of hot magma enabled magma bodies to rise to progressively shallower depths within the crust. This led to the development of mid- to upper-crustal magma reservoirs and subsequently, the Western and Eastern Redhills centres of the Skye central complex (EC1B, EC1C, EC1D and EC1E).

L1A lavas have previously been recognized as chemically and petrographically distinct from L3 and L2 lavas. All L1A lavas have been classified as Fe-poor intermediates by Thompson *et al.* (1972). Distinguishing petrographic features of Fe-poor lavas include the presence of plagioclase and magnetite phenocrysts, with rare-to-absent olivine. The least contaminated L1A samples come from the upper portion of the Beinn Edra stratigraphic group (Anderson & Dunham, 1966) and interdigitate with L3 lavas (Thompson *et al.*, 1972). This implies that the L1A reservoir existed contemporaneously with the L3 reservoir. More contaminated L1A samples all come from the upper portion of the Skye lava pile (Table 1), and, therefore, are also spatially distinct from L3 lavas.

The results are in agreement with previous conclusions that L1A magmas were contaminated in the lower crust (e.g. Dickin, 1981) and that AFC may have played a role in the production of some L1 samples (Thirlwall & Jones, 1983). Thompson *et al.* (1972) and Thompson (1974) proposed that the L1A magmas represent the daughter products of fractional crystallization of L3 magmas. Our results suggest that the L1A and L3 magmas are derived from distinct parental magmas.

The parental magmas of L1B and L1C samples are probably the end-products of EC1A, the RAFC event associated with L1A rocks. Model results suggest that L1B and L1C magmas evolved in separate but closely linked magma reservoirs. The presence of Eastern Redhills samples at the more evolved ends of the EC1B and EC1C indicates that periodic magmatic migrations from the magma reservoirs led first to the formation of the Western Redhills centre, and then to the formation of the Eastern Redhills centre. Samples from the basaltic

andesite facies of the Rubha'an Eireannaich composite sill (Table 1) plot on EC1C. However, samples from the rhyolite and intermediate portions of the sill plot away from the trend at  $^{87}\text{Sr}/^{86}\text{Sr}$  values similar to those of other Eastern Redhills intrusions. Additional EC-RAFC models are required to explain the genesis of these rocks. This phenomenon, in combination with compositional profiles for major and trace elements and Sr-isotopes that show continuous gradients between the ferrobasic andesite and rhyolite portions of the sill (Harker, 1904; Buist, 1959; Bell, 1983), provide evidence that the evolutionary histories of the Western and Eastern Redhills centres are linked. In addition, fine-grained acid inclusions within the Glamaig granite (Table 1) of L1B are petrographically and geochemically similar to inclusions within the Beinn an Dubhaich granite of the Outer Granite (Table 1) of the Eastern Redhills centre. Further evidence of a connection between the Western and Eastern Redhills centres is provided by Pb-isotopes, with the Eastern Redhills data extending from the range of Western Redhills values towards higher  $^{206}\text{Pb}/^{204}\text{Pb}$  and  $^{208}\text{Pb}/^{204}\text{Pb}$  (Fig. 2d).

EC-RAFC results EC1D and EC1E support the concept that L1D and L1E magmas originated from L1B and L1C parental magmas. The L1D and L1E reservoirs, which are probably shallower than the L1B and L1C reservoirs, were contaminated by LA-facies crust.

#### *Lineage 2: sublineages, model results and petrogenetic implications*

*L2: sublineages.* Lineage 2 rocks include the unlayered intrusions of the Cuillin centre (Table 1) and the PMB-type Skye lavas (Table 1). As noted above, the PMB lavas are compositionally similar to many Cuillin centre intrusions (Emeleus & Gyopari, 1992). The Cuillin centre has been proposed as a possible feeder for the PMB (Walker, 1993). The Cuillin centre is a composite layered intrusion of tholeiitic affinity (Table 1) consisting of a succession of layered and unlayered gabbroic and ultramafic intrusions, an acid intrusion and minor gabbroic intrusions. These intrude the Tertiary lava flows, T sandstones, and Jurassic sediments (Gass & Thorpe, 1976; Emelcus & Gyopari, 1992). An unnamed cone sheet suite (Table 1) is closely related in space and time to the Cuillin centre (Bell *et al.*, 1994). Some cone sheets within this suite cut the youngest intrusion of the Cuillin centre, but are older than the Western Redhills centre intrusions (Bell & Harris, 1986). In general, the cone sheets exhibit a typical tholeiitic Fe-enrichment trend and the least evolved members of the suite are similar in composition to the PMB lavas (Bell *et al.*, 1994). The focus of the present study is on the unlayered intrusions of the Cuillin centre because these rocks are interpreted as liquid compositions (e.g. Wager & Brown, 1968; Hutchison & Bevan, 1977; Dickin *et al.*, 1984).

The Coire Uaigneich Granophyre (CUG) is closely associated with the Cuillin centre in space and time and is chilled against Jurassic sediments. The same suite of cone sheets that cuts the layered rocks of the Cuillin centre also cuts the CUG. This provides strong evidence that the CUG is structurally related to the Cuillin centre (Bell & Harris, 1986; Emeleus & Gyopari, 1992), and hence it is included with the Cuillin centre in Table 1. According to Wager *et al.* (1953), the CUG crystallized under low-pressure conditions.

On the basis of radiogenic Pb-isotope variations, the data are divided into two sublineages for EC-RAFC analysis: L2A and L2B. On the  $^{206}\text{Pb}/^{204}\text{Pb}$  versus  $^{208}\text{Pb}/^{204}\text{Pb}$  diagram (Fig. 2d), the PMB-type Skye lavas, the Border Group (Table 1) and a dyke (Table 1) extend from values similar to the North Atlantic End Member (Ellam & Stuart, 2000) towards low  $^{206}\text{Pb}/^{204}\text{Pb}$ , but flat  $^{208}\text{Pb}/^{204}\text{Pb}$ . Compared with the PMB and Border Group rocks, the CUG (Table 1) data show high  $^{206}\text{Pb}/^{204}\text{Pb}$ .

*L2: model results.* EC-RAFC parameters and results for  $[\text{Sr}]$ - $^{87}\text{Sr}/^{86}\text{Sr}$  L2 data are displayed in Table 5 and Fig. 4. The presence of plagioclase phenocrysts requires that Sr is modelled as compatible in the magma in both EC2 simulations. The EC2A model requires an assimilant Sr-isotope ratio that is similar to that of LA-facies gneiss. L2B samples have high  $^{206}\text{Pb}/^{204}\text{Pb}$  in comparison with other L2A samples. High  $^{206}\text{Pb}/^{204}\text{Pb}$  values are a characteristic feature of T rocks (Fig. 2d; Dickin & Exley, 1981), and therefore assimilant compositional parameters are consistent with published values for T metasediments.

MELTS (Ghiorso, 1997) liquidus temperature calculations yield magma liquidus values of 1255°C at 1.5 kbar (upper-crustal depths) for the L2A samples with the lowest  $^{87}\text{Sr}/^{86}\text{Sr}$  values. The country-rock initial temperature and the local solidus temperature are consistent with the thermal characteristics of leucocratic to mesocratic amphibolite gneiss (Thompson, 1981). The magma thermal and geochemical characteristics in the EC2B model are similar to those of the most radiogenic samples of EC2A. In the EC2B model, the local solidus temperature is similar to that of T metasediments and leucocratic LA gneiss (Thompson, 1981). The initial wall-rock temperature for EC2B is higher than that of EC2A. The CUG (in L2B) is located in the Cuillin centre and T rocks in the vicinity show evidence of being thermally metamorphosed and partially melted by previously emplaced Cuillins gabbros (L2A); therefore, it is possible that the relatively high EC2B wall-rock temperature reflects the previous intrusive history.

Three episodes of recharge are modelled in EC2A and two recharge episodes are modelled in EC2B. In both models, the  $^{87}\text{Sr}/^{86}\text{Sr}$  value of recharge magma is higher

than that of the uncontaminated host magma, which may indicate that recharge magma underwent RAFC prior to addition to host magma. In addition, Sr is compatible in the recharge magma—in EC2A, the Sr-bulk distribution coefficient is modelled to increase with falling temperature.

The proportion of anatectic melt that is assimilated is greater in EC2A ( $\lambda = M_a^*/M_a^o = 0.99$ ) than in EC2B ( $\lambda = M_a^*/M_a^o = 0.41$ ). This is because the EC2A magma liquidus temperature ( $T_{l,m}$ ) is relatively high and more heat is generated during cooling and crystallization of the magma. Also, the EC1B equilibration temperature ( $T_{eq}$ ) is closer to the solidus (Table 5); therefore, the melt productivity of the wall rock is smaller and the wall-rock melts to a smaller degree. The ratio of mass of assimilated melt to mass of cumulates removed is similar in both models (EC2A:  $M_a^*/M_c = 1.55$ ; EC2B:  $M_a^*/M_c = 1.45$ ).

*L2: petrogenetic implications of EC-RAFC results.* L2A magmas evolved via RAFC processes within a middle- to upper-crustal magma chamber. Derivatives of these (L2B) ascended to the uppermost portion of the crust and assimilated T metasediments.

The EC2B model results are consistent with the conclusion of Dickin & Exley (1981), that the CUG (Table 1) originated from mixing of partially melted T sediments and L2A-type magma. The results also support the conclusions of Bell *et al.* (1994) that the parental magma to the Cuillin cone sheet suite (L2A) is of PMB type, that the most primitive cone sheets show little evidence of crustal contamination, and that the more evolved cone sheet magmas were generated from the primitive magmas by AFC processes. In addition, the results confirm the long-held view (e.g. Thompson *et al.*, 1972) that the PMB and SMLS magma types of the Skye lava succession have different parental liquids.

### *Lineage 3: sublineages, model results, and petrogenetic implications*

*L3: sublineages.* Lineage 3 samples are mainly olivine and plagioclase-phyric basalts of SMLS type (Thompson *et al.*, 1972). The data are divided into three sublineages: L3A, L3B and L3C, on the basis of Sr–Pb concentration and isotope characteristics (Fig. 5).

In L3A and L3B, radiogenic Pb- and Sr-isotope trends are approximately vertical or negatively correlated (Fig. 5a). This relationship is reversed in L3C, where the isotope–isotope trend is distinctly positive. In all three sublineages, the  $[\text{Sr}]$  versus  $^{87}\text{Sr}/^{86}\text{Sr}$  data (Fig. 5b) form saw-tooth patterns. Given constraints on likely assimilants, these trends—a common feature of the Skye dataset—are difficult to explain by fractional crystallization and assimilation processes alone. In a number of cases, MgO and Sr concentrations increase whereas  $^{87}\text{Sr}/^{86}\text{Sr}$  and  $^{206}\text{Pb}/^{204}\text{Pb}$  remain relatively constant.

Table 5: EC-RAFC parameters, Lineage 2

Thermal parameters	EC2A	EC2B
Magma liquidus temperature, $T_{l,m}$	1255° C	1060° C
Magma initial temperature, $T_m^\circ$	1255° C	1060° C
Assimilant liquidus temperature, $T_{l,a}$	1030° C	950° C
Assimilant initial temperature, $T_a^\circ$	170° C	500° C
Recharge magma liquidus temperature, $T_{l,r}$	1220° C	1055° C
Recharge magma initial temperature, $T_r^\circ$	1220° C	1055° C
Solidus temperature, $T_s$	730° C	715° C
Equilibration temperature, $T_{eq}$	1041° C	835° C
Crystallization enthalpy, $\Delta h_m$ (J/kg)	396000	350000
Isobaric specific heat of magma, $C_{p,m}$ (J/kg K)	1484	1400
Fusion enthalpy, $\Delta h_a$ (J/kg)	330000	300000
Isobaric specific heat of assimilant, $C_{p,a}$ (J/kg K)	1400	1370
Crystallization enthalpy of recharge magma, $\Delta h_r$ (J/kg)	396000	350000
Isobaric specific heat of recharge magma, $C_{p,r}$ (J/kg K)	1484	1350
Mass of recharge magma		
Recharge episode 1	0-80, 1126° C	1-80, 955° C
Recharge episode 2	0-15, 1080° C	0-25, 870° C
Recharge episode 3	0-63, 1070° C	
<i>Compositional parameters</i>		
	Sr	Sr
Magma initial concentration (ppm), $C_m^\circ$	113	239
Magma isotope ratio, $\epsilon_m^\circ$	0-70300	0-70744
Magma trace-element distribution coefficient, $D_m$ , and range	1, 1-88–2-08	1-45, 2-08–2-24
Enthalpy of trace-element distribution reaction, $\Delta H_m$	–8000	–4000
Assimilant initial concentration (ppm), $C_a^\circ$	540	199
Assimilant isotope ratio, $\epsilon_a^\circ$	0-71050	0-73519
Assimilant trace-element distribution coefficient, $D_a$ , and range	0-28, 0-83–0-41	0-65
Enthalpy of trace-element distribution reaction, $\Delta H_a$	–4000	—
Recharge magma initial concentration (ppm), $C_r^\circ$	200	260
Recharge magma isotope ratio, $\epsilon_r^\circ$	0-70315	0-71200
Recharge magma trace-element distribution coefficient, $D_{m,r}$ , and range	0-10, 1-06–1-56	1-80
Enthalpy of trace-element distribution reaction, $\Delta H_r$	–30000	—
<i>Mass characteristics</i>		
Mass of assimilant partial melt, $M_a^*$	0-73	1-35
Mass of cumulates, $M_{ct}$	0-47	0-93
Mass of recharge magma, $M_r^\circ$	1-58	2-05
Mass of country rock involved in RAFC event, $M_a^\circ$	0-74	3-3

One interpretation of these characteristics is that the magmatic system is characterized by multiple recharge events. The hypothesis that L3A, L3B and L3C are the result of complex RAFC processes is tested below, through EC-RAFC modelling of  $[Sr]^{-87}Sr/^{86}Sr$  and  $^{87}Sr/^{86}Sr-^{206}Pb/^{204}Pb$  data.

*L3: model results.* Table 6 shows input parameters for L3  $[Sr]^{-87}Sr/^{86}Sr$  and  $^{87}Sr/^{86}Sr-^{206}Pb/^{204}Pb$  EC-RAFC

simulations. Sr is modelled as compatible in the magma in all three EC3 simulations because of the ubiquity of plagioclase as a phenocryst phase. In L3A, there is a broad increase in the abundance of plagioclase phenocrysts with increasing  $^{87}Sr/^{86}Sr$ , so the bulk distribution coefficient for Sr in EC3A was modelled to become more compatible with falling temperature. Data from L3A and L3B show a vertical or negative correlation between Pb- and Sr-isotopic values, which is consistent with

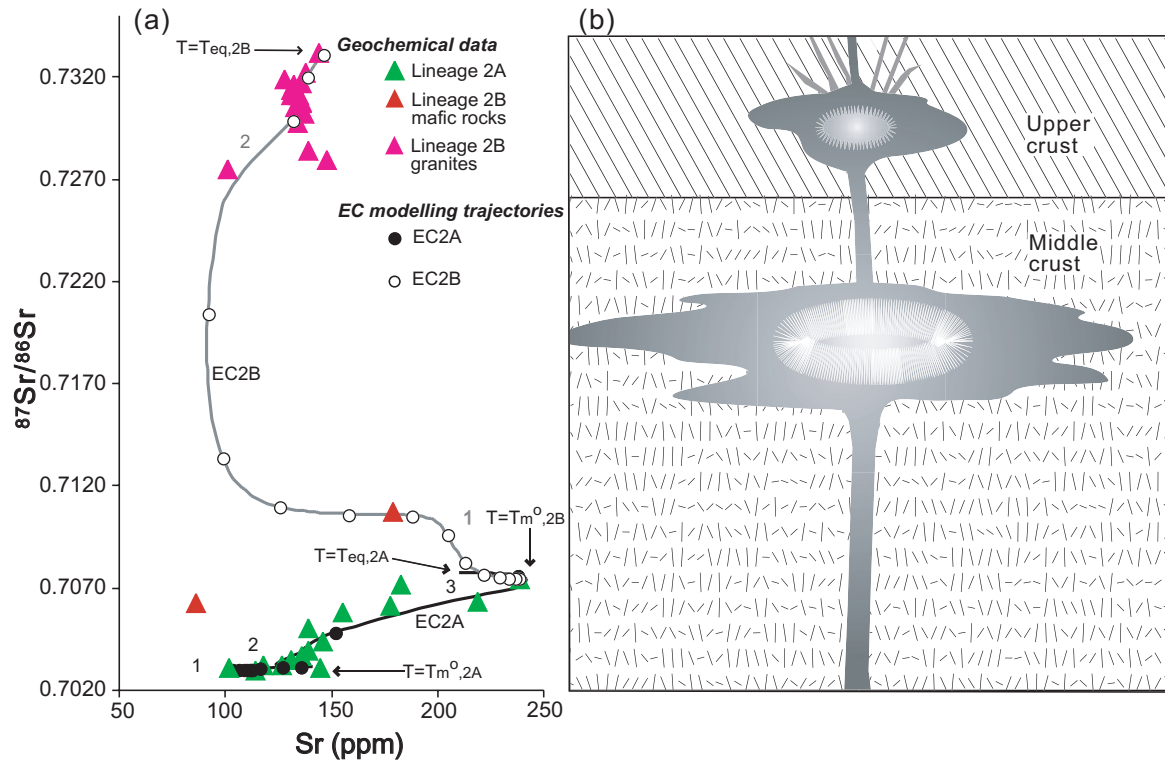


**Fig. 4.** (a) Plot of [Sr] ppm versus initial  $^{87}\text{Sr}/^{86}\text{Sr}$  data (PMB lavas, Cuillin centre intrusion; see Fig. 2 for data references) and results of EC-RAFC simulations (EC2A and EC2B) for lineages L2A and 2B. Temperature drop for each symbol of EC-RAFC trends:  $18.3^\circ\text{C}$  (EC2A),  $16.0^\circ\text{C}$  (EC2B). Numbers on EC-RAFC trends show recharge episodes, and arrows represent direction of falling magma temperature. (b) Schematic diagram of possible L2 magmatic system. Table 5 shows recharge magma masses and temperatures of addition.

interaction with LG (see Fig. 2b and c). The modelled country-rock Sr concentration and Sr- and Pb-isotope values therefore correspond to published values for LG-facies gneiss (Weaver & Tarney, 1980; Whitehouse, 1990). The required input country-rock isotope and concentration values are typical of an intermediate to mafic lithology. This may be consistent with a negative to flat  $\text{MgO}-^{87}\text{Sr}/^{86}\text{Sr}$  correlation—the assimilant is unlikely to have added MgO because its MgO concentration is similar to that of the host magma. The magma chambers probably resided in the lower to middle crust. In EC3C, the assimilant has relatively radiogenic Sr- and Pb-isotopic values in comparison with EC3A and EC3B. These more radiogenic values are consistent with an assimilant of middle- to upper- crustal LA-facies (LA) gneiss. A contamination site within the middle- to upper-crust is consistent with incorporation of such an assimilant. Sr is incompatible in the country rock in all three EC3 models.

To calculate an initial magma liquidus temperature for EC3A, we used the MELTS simulator (Ghiorso, 1997)—a thermodynamically based model of crystal–melt equilibria. We selected sample SK 940 (Thompson *et al.*, 1972) for MELTS analysis because it has the lowest  $^{87}\text{Sr}/^{86}\text{Sr}$

value in L3A (0.70308). This sample has 593 ppm Sr and 8.11 wt % MgO. The MELTS simulator calculated a liquidus temperature of  $1396^\circ\text{C}$ , which is based on a pressure of 1.4 GPa (upper-mantle–lower-crustal depths). The thermal and geochemical parameters for the initial magma of EC3B are those of the final magma for EC3A. In EC3A and EC3B, the country-rock thermal parameters correspond to typical values for an intermediate to mafic lithology, as proposed above. The starting parameters for the initial magma of EC3C correspond to the final magma of EC3B, and country-rock thermal parameters are consistent with a location at relatively shallow crustal levels.

Based on  $\text{Sr}-^{87}\text{Sr}/^{86}\text{Sr}$ ,  $\text{MgO}-^{87}\text{Sr}/^{86}\text{Sr}$  and  $^{87}\text{Sr}/^{86}\text{Sr}$ –radiogenic Pb-isotopic correlations, six episodes of recharge are modelled in EC3A and two episodes of recharge are modelled in EC3B. One episode of recharge is required in EC3C to explain L3C data. Recharge episodes are labelled in Fig. 5b, and Table 6 shows the temperature and relative mass of recharge magma added during each of the recharge ‘events’. The theoretical trends that best fit observed L3 data require model parameters in which recharge magma has progressively higher initial  $^{87}\text{Sr}/^{86}\text{Sr}$  and lower initial

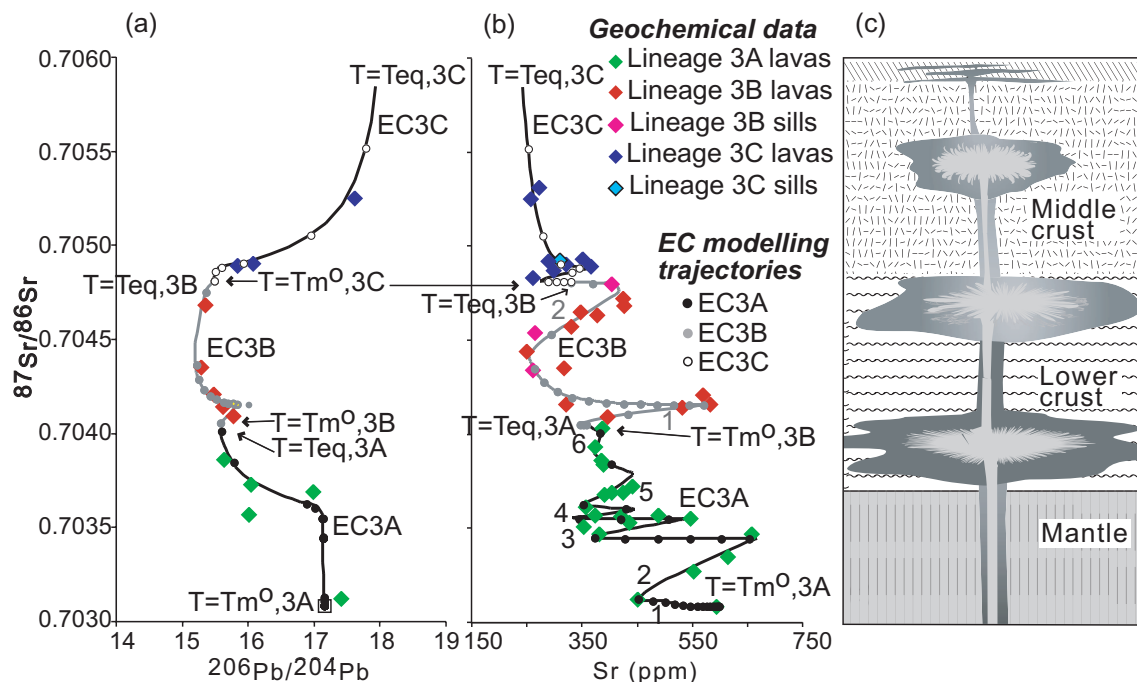


**Fig. 5.** (a) Plot of  $^{206}\text{Pb}/^{204}\text{Pb}$  versus  $^{87}\text{Sr}/^{86}\text{Sr}$  data and EC-RAFC trends (EC3A, EC3B and EC3C) for lineages 3A, 3B and 3C. (b) [Sr] ppm versus  $^{87}\text{Sr}/^{86}\text{Sr}$  data (SMLS lavas from the lower part of the Skye lava succession, Little Minch Sill Complex sills; see Fig. 2 for data references) and results of EC-RAFC simulations (EC3A, EC3B and EC3C) for lineages L3A, L3B and L3C. Temperature drop for each symbol of the EC-RAFC trend: 3–4°C (EC3A), 7–5°C (EC3B), 5–5°C (EC3C). Numbers on EC-RAFC trends show recharge episodes, and arrows represent direction of falling magma temperature. (c) Schematic diagram of possible L3 magmatic system. Table 6 shows recharge magma masses and temperatures of addition.

$^{206}\text{Pb}/^{204}\text{Pb}$  ratios than melt already residing in the magma body. In addition, recharge episodes generally coincide with increasing MgO and Sr concentrations. If the mantle source of the recharge magma is the same as that of the minimally contaminated melt within the magma body, the recharge magma probably underwent some assimilation prior to intrusion into the magma body. Based on this assumption, the high Sr concentration required for recharge magma suggests that plagioclase is not a stable liquidus phase in recharge magma. Sr is therefore modelled as incompatible in the recharge magma in EC3A and EC3B. Compatibility gradually increases, and Sr is compatible in the recharge magma in EC3C. An alternative explanation for the composition of the recharge magma is that it may be derived from a mantle source region compositionally distinct from that of earlier partial melting episodes.

When the first pulse of recharge magma (labelled '1' on EC3A, EC3B and EC3C, Fig. 5b) is introduced,  $^{87}\text{Sr}/^{86}\text{Sr}$  increases because the Sr-isotope composition of the recharge magma is slightly more radiogenic than that of the host magma. However, in EC3A, the  $^{206}\text{Pb}/^{204}\text{Pb}$  value of the recharge magma is similar to that of the host magma (Table 6), leading to a virtually vertical trajectory in  $^{206}\text{Pb}/^{204}\text{Pb}$ – $^{87}\text{Sr}/^{86}\text{Sr}$  space (Fig. 5a). In EC3B, the recharge magma  $^{206}\text{Pb}/^{204}\text{Pb}$  is similar to that

of the host magma, which leads to an approximately flat  $^{206}\text{Pb}/^{204}\text{Pb}$  trend. In EC3C, the recharge magma is relatively radiogenic, and recharge causes an increase in  $^{206}\text{Pb}/^{204}\text{Pb}$  in melt within the magma body.

Sr is compatible in all three EC3 magma bodies, so [Sr] initially decreases as country rock is heated to the solidus from its initial temperature [see Bohron & Spera (2001) for further explanation of this phenomenon]. In EC3B, recharge (designated by '1' and '2' on EC3B, Fig. 5b) leads to an increase in [Sr] because Sr is incompatible in the recharge magma. In contrast, although [Sr] in EC3A is relatively high and the element behaves incompatibly in the recharge magma, [Sr] does not increase during the first recharge episode. This is because the mass of recharge magma is relatively small and because Sr is highly compatible in the host magma. Subsequent additions of recharge magma in EC3A and EC3B (Fig. 5b) lead to increases in host magma of both [Sr] and  $^{87}\text{Sr}/^{86}\text{Sr}$  because the proportions of recharge magma are relatively large. In EC3C (Fig. 5b), even though Sr is compatible in the recharge magma, [Sr] of melt in the host magma body increases during the recharge episode ('1' on EC3C, Fig. 5b) because [Sr] of recharge magma is relatively high. In all EC3 models, Sr is incompatible in the country rock. Despite this, when the magmatic system is dominated by fractional crystallization and assimilation

Table 6: EC-RAFC parameters, Lineage 3

Thermal parameters	EC3A	EC3B	EC3C			
Magma liquidus temperature, $T_{l,m}$	1400°C	1220°C	1100°C			
Magma initial temperature, $T_m^\circ$	1400°C	1170°C	1040°C			
Assimilant liquidus temperature, $T_{l,a}$	1370°C	1180°C	1170°C			
Assimilant initial temperature, $T_a^\circ$	630°C	620°C	350°C			
Recharge magma liquidus temperature, $T_{l,r}$	1370°C	1360°C	1130°C			
Recharge magma initial temperature, $T_r^\circ$	1370°C	1360°C	1130°C			
Solidus temperature, $T_s$	1040°C	845°C	850°C			
Equilibration temperature, $T_{eq}$	1171°C	1037°C	995°C			
Crystallization enthalpy, $\Delta h_m$ (J/kg)	396000	396000	396000			
Isobaric specific heat of magma, $C_{p,m}$ (J/kg K)	1484	1484	1484			
Fusion enthalpy, $\Delta h_a$ (J/kg)	420000	420000	370000			
Isobaric specific heat of assimilant, $C_{p,a}$ (J/kg K)	1550	1530	1390			
Crystallization enthalpy of recharge magma, $\Delta h_r$ (J/kg)	396000	396000	396000			
Isobaric specific heat of recharge magma, $C_{p,r}$ (J/kg K)	1480	1480	1480			
Mass and temperature of recharge magma						
Recharge episode 1	0.03, 1300°C	0.80, 1147°C	0.80, 1018°C			
Recharge episode 2	0.68, 1280°C	0.80, 1049°C				
Recharge episode 3	0.59, 1230°C					
Recharge episode 4	0.50, 1203°C					
Recharge episode 5	0.44, 1189°C					
Recharge episode 6	0.13, 1176°C					
<i>Compositional parameters</i>						
	Sr	Pb	Sr	Pb	Sr	Pb
Magma initial concentration (ppm), $C_m^\circ$	600	3.4	358	1.63	330	3.38
Magma isotope ratio, $\epsilon_m^\circ$	0.70308	17.16	0.70405	15.59	0.70481	15.49
Magma trace-element distribution coefficient, $D_m$ , and range	1	0.60	1.57	0.5	2.26	0.70
	1.98–2.21	2.19–2.27				
Enthalpy of trace-element distribution reaction, $\Delta H_m$	–9500	—	–4000	—	—	—
Assimilant initial concentration (ppm), $C_a^\circ$	200	0.2	235	0.4	250	7
Assimilant isotope ratio, $\epsilon_a^\circ$	0.70453	12	0.70517	12	0.71200	19.5
			<i>EC3A</i>	<i>EC3B</i>	<i>EC3C</i>	
Assimilant trace-element distribution coefficient, $D_a$ , and range	0.12, 0.59–0.33	0.05	0.06, 0.45–0.24	0.01	0.60	0.07
Enthalpy of trace-element distribution reaction, $\Delta H_a$	–12000	—	–15000	—	—	—
Recharge magma initial concentration (ppm), $C_r^\circ$	955	0.2	1100	5	700	0.25
Recharge magma isotope ratio, $\epsilon_r^\circ$	0.70363	16.9	0.70422	16	0.70494	16.5
Recharge magma trace element distribution coefficient, $D_r$ , and range	0.05	0.40	0.89	0.30	1.30	0.50
			0.59–0.89			
Enthalpy of trace-element distribution reaction, $\Delta H_r$	–35000	—	—	—	—	—
<i>Mass characteristics</i>						
Mass of assimilant partial melt, $M_a^*$	0.42		1.17		0.10	
Mass of cumulates, $M_{ct}$	0.91		0.68		0.52	
Mass of recharge magma, $M_r^\circ$	2.37		1.60		0.80	
Mass of country rock involved in RAFC event, $M_a^\circ$	2.4		2.0		0.6	

(i.e. in between recharge 'events'), [Sr] decreases. This is a result of the strong compatibility of Sr in the melt coupled with the low [Sr] of the assimilant.

The relative mass of recharge magma added to the magmatic system decreases steadily from EC3A to EC3B and to EC3C (Table 6). Such a result may be consistent with the increasingly differentiated nature of the recharge magma suggested by its increasing Sr-isotope signatures. The proportion of anatectic melt that is assimilated is smaller in EC3C ( $\lambda = M_a^*/M_a^o = 0.17$ ) than in EC3A ( $\lambda = M_a^*/M_a^o = 0.18$ ) and EC3B ( $\lambda = M_a^*/M_a^o = 0.59$ ). In EC3C, more heat is required to elevate the low initial country-rock temperature ( $T_a^o$ ) to the solidus temperature ( $T_s$ ), so assimilation begins at a lower  $T_m$  (Table 6). The EC3B  $\lambda$  is larger than in EC3A because of the high  $T_{l,a}$  of the EC3A model. The ratio  $M_a^*/M_c$  is lowest in EC3A, reflecting the high solidus temperature.

When anatectic melt is mixed into the magma bodies,  $^{87}\text{Sr}/^{86}\text{Sr}$  becomes markedly more radiogenic as a result of the incorporation of  $^{87}\text{Sr}/^{86}\text{Sr}$ -rich assimilant. The generally negative  $^{87}\text{Sr}/^{86}\text{Sr}$ - $^{206}\text{Pb}/^{204}\text{Pb}$  trajectory in EC3A and EC3B is because of the incompatible behaviour of Pb in the country rock and the low  $^{206}\text{Pb}/^{204}\text{Pb}$  value of the anatectic melt (LG), but because LA crust has relatively high  $^{206}\text{Pb}/^{204}\text{Pb}$ , assimilation leads to significantly more radiogenic  $^{206}\text{Pb}/^{204}\text{Pb}$  values in EC3C.

*L3: petrogenetic implications of EC-RAFC results.* The [Sr]- $^{87}\text{Sr}/^{86}\text{Sr}$  and  $^{87}\text{Sr}/^{86}\text{Sr}$ - $^{206}\text{Pb}/^{204}\text{Pb}$  continuity in the L3 data together with modelling results consistently indicate that the assimilant composition changed from lower-crustal LG to middle- to upper-crustal LA. This, in turn, suggests that L3 magma reservoirs progressively ascended to higher levels in the crust. We note also that the average value of  $\lambda$  ( $\equiv M_a^*/M_a^o$ ), a measure of the importance of partial melting and contamination (N.B.  $\chi = 1$ ) is 0.31, which is relatively high, indicative of profound chemical contamination. The mean  $M_r$  for the L3 trajectories (EC3A, EC3B and EC3C) is 1.6, clearly showing, once again, the thermal connection between recharge, country-rock partial melting and concomitant chemical contamination of L3 Skye magmas.

The high (in comparison with host magma)  $^{87}\text{Sr}/^{86}\text{Sr}$  and low  $^{206}\text{Pb}/^{204}\text{Pb}$  values required for recharge magma in the EC3 models suggest that recharge magma itself underwent AFC before intrusion into the host magma. In EC3A, the first recharge event takes place before the composition of the magma body has been affected by assimilation. During this interval, MgO shows a strong positive correlation with  $^{87}\text{Sr}/^{86}\text{Sr}$ . The trend towards high MgO contents in the host magma during recharge 'events' probably indicates that the MgO content of the recharge magma was higher than that of the magma intruded and is consistent with a flux of replenishment

magma newly arrived from the deeper part of the sub-crustal lithosphere.

Our conclusions that the L3 magmas reservoirs shoaled with time and that RAFC processes are important in the evolution of the magmas differ from those of Thompson *et al.* (1982) and Thirlwall & Jones (1983). Because these workers observed no correlation between the amount of contamination and the extent of fractionation, they suggested that any crustal contamination occurred after fractional crystallization. Our results are also inconsistent with the model of Dickin *et al.* (1984), who suggested that contamination of magma batches took place within a plexus of narrow sills. However, because only one EC-RAFC trend is required to explain L3A, L3B and L3C data, the results support the conclusion of Gibson & Jones (1991) that the Little Minch sills (Table 1) and the SMLS-type Skye lavas evolved in the same, or a set of closely related, magma reservoirs.

## DISCUSSION

### Interpretation of EC-RAFC modelling results

Within the diverse rocks of the Skye Tertiary igneous centre, we have identified three main petrologic lineages and 10 sublineages that are related chemically, spatially and temporally. Using the EC-RAFC simulator, we have constructed self-consistent RAFC scenarios (modelling trajectories) to explain observed Pb- and Sr-isotope systematics and Sr abundances in terms of assimilation, recharge and fractional crystallization. In this section, we examine the significance of the results with respect to the evolution of the entire magmatic system.

Our interpretation is that the Skye igneous centre is characterized by three distinct parental magmas (initial magma compositions for trajectories EC1A, EC2A and EC3A) that evolved via open-system RAFC processes. A critical outcome of our modelling is that among the magmatic derivatives within individual lineages, the end-product of one EC-RAFC trajectory serves as the starting condition for a subsequent magma evolutionary phase represented by younger rocks (e.g. EC2A  $\rightarrow$  EC2B). In addition, models that best fit the observed data utilize thermal and chemical parameters that implicate assimilation of wall rock from progressively shallower parts of the crust. This suggests that, with time, the Skye magmatic storage and transport system matured by establishing new magma reservoirs at progressively shallower depths. In this respect, our results are consistent with, and serve to quantify, the MASH process proposed by Hildreth & Moorbath (1988). In the case where the assimilant was modelled as, for example, LG, input parameters for each lineage required distinct compositional and thermal parameters, which

highlight the heterogeneous and stratified nature of the crust of western Scotland in the Tertiary.

Another conclusion to be drawn from the modelling results is that the composition and enthalpy per unit mass, as reflected in the temperature of the recharge magma, also evolved in time and space. Distinct recharge magmas characterize each sublineage, but for each lineage, where the modelling suggests that the magmatic reservoirs progressively ascended to higher crustal levels, best-fit results require recharge magmas of more evolved composition and lower specific enthalpy. It is possible, although in our opinion unlikely, that the distinctions in recharge magmas result from complex melting processes in a heterogeneous mantle. On the other hand, if the recharge magmas themselves are the products of RAFC processes, two interesting questions beyond the scope of this study arise: What are the origins (i.e. RAFC histories) of these recharge magmas? And what are the temporal and physical relationships between the 'recharge' magma reservoirs and the host magma reservoirs?

Results of EC-RAFC modelling yield the mass of thermally involved country rock ( $M_a^o$ ), assimilant ( $M_a^*$ ), cumulates ( $M_c$ ), and recharge magma ( $M_r$ ), each normalized to the initial mass of the host magma reservoir ( $M_o$ ) for a given RAFC trajectory. Table 6 shows these parameters for each trajectory. One notable feature is that the 'parental' trajectories EC1A, EC2A and EC3A are characterized by values for  $M_a^o$ ,  $\lambda$  and  $M_r$  that are higher than mean values averaged over all trajectories. This suggests that the parental sublineages were most influenced by open-system behaviour (contamination and recharge), although virtually all sublineages, with the possible exception of EC1E, exhibit open-system behaviour ( $M_a^*$ ,  $M_r > 0$ ). A positive correlation exists between assimilation mass,  $M_a^*$ , and recharge mass,  $M_r$ . The mechanism driving the correlation is obvious; additional heat from recharge magma heat is available for country-rock anatexis. Within lineages L1 and L3, the mass of recharge magma for successive trajectories decreases quasi-monotonically with time. An exception is L2, although, even there,  $M_r$  was approximately constant during EC2A  $\rightarrow$  EC2B evolution.

Because Skye is the most complex natural system to which the EC-RAFC model has been applied in detail, comparisons with other natural systems cannot yet be made. However, if these ranges of assimilant and recharge masses are supported by further work, the results suggest that magmatic systems can be influenced by relatively large masses of assimilant and recharge melts. RAFC modelling results are consistent with the integrated mean ratio of intrusive to extrusive magma mass of  $\sim 5$ . Similarly, inferences drawn from RAFC geochemical modelling that unequivocally point to significant magma recharge during the magmatic evolution at Skye are consistent with material–energy

balance estimates provided in an earlier section of the present study.

### Implications for the stratigraphy of the Skye Igneous Centre

Figure 6 is a schematic illustration of the Skye magmatic transport and storage systems. The oldest rocks are Skye lavas of SMLS transitional alkali basalt-type that belong to L3, and RAFC modelling suggests that the associated reservoirs initially resided at lower-crustal depths, perhaps close to the seismic Moho (Fig. 6). Flow-by-flow stratigraphic data on the Skye lavas are scarce, so details of the temporal significance of the Skye lava EC-RAFC results are not resolved here. However, there are broader stratigraphic and geochemical implications. For L3, the presence of Little Minch Sill Complex sills (Table 3) in L3B and L3C, but not in L3A, suggests that L3 magmas underwent RAFC processes at progressively higher levels in the crust (Fig. 6b). The stratigraphically oldest rocks in L1 appear to be associated with a magma reservoir that resided at higher levels in the crust than the earliest rocks from L3. There is evidence that the oldest L1 rocks are slightly younger than those of L3 and, therefore, perhaps the higher-level magma reservoir reflects the same type of system maturation that is implicated by results of L3.

The next phase of igneous activity involved the end of flood basalt volcanism and the emplacement of the Outer Unlayered Gabbro (Table 1) of L1B at the future site of the Cuillin centre (L2). Rocks of L2 were emplaced during a pause in L1 igneous activity. The L2A magma reservoir developed at a higher level in the crust than the earliest L3 or L1 reservoirs, and the L2B reservoir then formed in the uppermost crust. The development of these high-level magma chambers may have been facilitated by earlier heating of the crust by L1 magmas.

The last major phase of igneous activity involved the formation of the granitic centres (L1B, L1C, L1D and L1E). There is evidence that the stratigraphically oldest rocks of the Western Redhills centre in L1B (Table 1) and L1C (Table 1) evolved concurrently, but underwent distinct RAFC episodes. Intermingling of the L1B and L1C liquids produced a suite of mixed rocks (Table 1). The L1D and L1E reservoirs formed in the upper crust at higher levels than those of L1B. Our interpretation is that these higher-level magma reservoirs reflect system maturation not unlike that indicated by lineages L2 and L3.

### SUMMARY AND CONCLUSIONS

In this study, we have presented evidence that the EC-RAFC formulation can reasonably capture complex geochemical trends and provide quantitative (or semi-quantitative) constraints on material balance (e.g. mass of assimilant, mass of recharge, mass of cumulates, etc.) and concomitant energy requirements. Interestingly, the

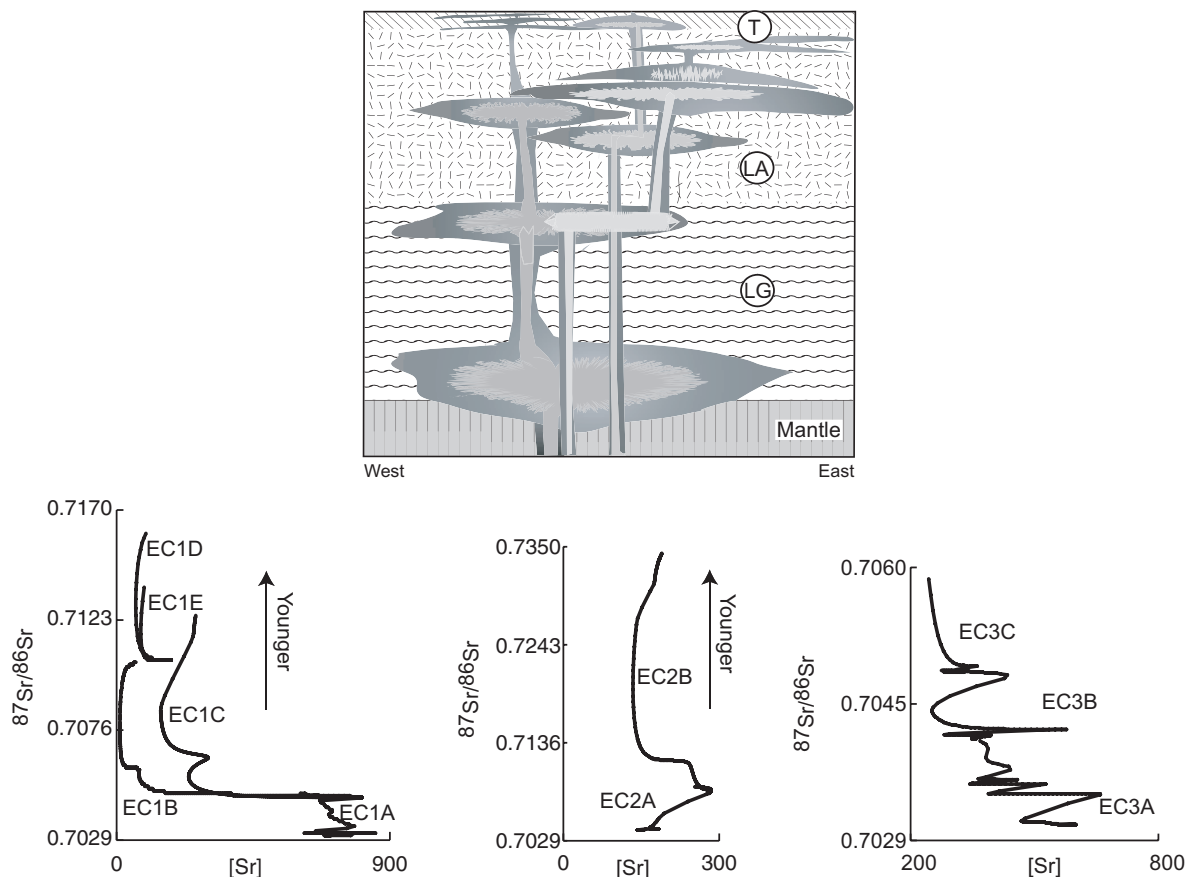


**Fig. 6.** Schematic illustration of a possible Skye magmatic plumbing system based on the results of EC-RAFC models. Based on stratigraphic data for SMLS lavas and intrusions associated with the Western and Eastern Redhills centres (L1), and PMB lavas and intrusions of the Cuillin centre (L2), temporal relations within L1 and L2 are indicated (see EC-RAFC plots below illustration). Detailed stratigraphic data on the Skye lavas (L3) are scarce, so the temporal significance of the EC-RAFC results is not resolved here on a flow-by-flow basis. However, the results are broadly consistent with the development of magma reservoirs at progressively higher levels in the crust. Abbreviations as in Figs 2 and 3.

EC-RAFC-derived balances are entirely consistent with mass and transport estimates based on regional 'geophysical' inferences. Hence, the EC-RAFC model provides a link between the geochemistry of intrusive, hypabyssal and extrusive rocks and broad-scale regional tectonics. This connection provides a powerful predictive tool for formulating insightful questions about magma dynamics, the transport of magma and magmatic heat and the local crustal growth rate in regions undergoing extension or extensional shear failure.

Our results provide strong evidence that the Skye magma storage and transport system was spatially complex and evolved thermally and compositionally. Previous workers have attributed the compositional variations in Skye magmas to different mantle sources and an array of disconnected shallow-level processes. In contrast, the results that we have presented show that the evolution of the Skye magmatic system can be modelled parsimoniously, provided the inherently non-linear coupling between assimilation, recharge and fractional

crystallization are self-consistently accounted for. That is, Skye magmas derive from a relatively small number of parental magmas exhibiting relatively limited compositional variation. The wide compositional range of derivative magmas forms by various combinations of fractional crystallization, magma recharge and assimilation of anatectic melts. Our results suggest, therefore, that at least to a first approximation, the complex geochemical signatures observed at Skye can be explained without recourse to lithospheric source heterogeneity (a very difficult hypothesis to test), complications because of varying environmental conditions of partial melting and ascent, selective movement of trace elements in a fluid phase during anatexis, and special contaminants. A critical outcome of our quantitative modelling is that the character of the crustal assimilant affecting the magmatic products of the Skye igneous centre changes systematically. In general, lower-crustal granulite is the contaminant for the early-formed magmas, middle- to upper-crustal amphibolite is the contaminant for magmas formed

during the intermediate stages of magmatism, and upper-crustal metasediments act as the contaminant for many of the late-stage magmas. The ambient crustal temperature changes from hotter in the cases where lower-crustal melts are assimilated to cooler in the cases where upper-crustal melts are the contaminants in accord with geothermal gradients. Such systematic changes in indicators of crustal residence levels strongly indicate that the associated magma reservoirs progressively shoaled as each magmatic lineage and its collection of sub-systems matured. The models presented here are sensitive to the input parameters, and all of the parameters are geologically relevant and reasonable. The critical point is that by comparing theoretical energy-constrained results with observed data trends, a set of parameters describing the physicochemical state of the relevant magma system emerges. In this study, a crustal-scale pattern of magmatic activity is implied by our results, and numerous additional petrologic and geochemical data can now be used to test and further refine our hypothesis.

One can view the Tertiary magmatic system at Skye, or indeed, any open RAFC magmatic system, as a large-scale dissipative structure (e.g. see Nicolis & Prigogine, 1977) exhibiting features of self-organization through time. The sustained input of  $\sim 0.2$  GW of heat for  $\sim 7$  Myr is the mechanism driving the system. The processes of assimilation, recharge and fractional crystallization are non-linearly coupled to one another via the RAFC conservation equations. Entropy production associated with the dissipation of magmatic heat in the Earth's gravitational field naturally leads to the upward shoaling of transgressive magmatic centres at Skye, with concomitant evolution of magma composition and volume and net growth of continental crust.

## ACKNOWLEDGEMENTS

Reviews by Jeremy Preston, Mary Reid, an anonymous reviewer and editor Marjorie Wilson greatly improved the form and content of this work and are gratefully acknowledged. Support from the National Science Foundation to W.A.B. (NSF EAR-0073883) and F.J.S. (NSF EAR 0073932) is gratefully acknowledged. F.J.S. acknowledges additional support from the US Department of Energy Geosciences Program (Nick Woodward) DE-FG03-01ER15210. This work represents the Masters thesis of S.J.F.

## REFERENCES

- Anderson, F. W. & Dunham, K. C. (1966). The geology of northern Skye. *Memoirs of the Geological Survey*. London: HMSO.
- Bailey, E. B., Clough, C. T., Wright, W. B., Richey, J. E. & Wilson, G. V. (1924). Tertiary and post-Tertiary geology of Mull, Loch Aline and Oban. *Memoir of the Geological Survey, Great Britain*. London: HMSO.
- Bamford, D., Nunn, K., Prodehl, C. & Jacob, B. (1977). LISP-III: upper crustal structure of northern Britain. *Journal of the Geological Society, London* **133**, 481–488.
- Beckinsale, R. D., Pankhurst, R. J., Skelhorn, R. R. & Walsh, J. N. (1978). Geochemistry and petrogenesis of the Early Tertiary lava pile of the Isle of Mull, Scotland. *Contributions to Mineralogy and Petrology* **66**, 415–427.
- Bell, J. D. (1976). The Tertiary intrusive complex on the Isle of Skye. *Proceedings of the Geologists' Association* **87**, 247–271.
- Bell, B. R. (1983). Significance of ferrodioritic liquids in magma mixing processes. *Nature* **306**, 323–327.
- Bell, B. R. & Harris, J. W. (1986). *An Excursion Guide to the Geology of the Isle of Skye*. Geological Society of Glasgow, 317 pp.
- Bell, B. R. & Pankhurst, R. J. (1993). Sr-isotope variations in a composite sill: crystal–liquid processes and the origin of the Skye granites. *Journal of the Geological Society, London* **150**, 121–124.
- Bell, B. R., Claydon, R. V. & Rogers, G. (1994). The petrology and geochemistry of cone-sheets from the Cuillin Igneous Complex, Isle of Skye: evidence for combined assimilation and fractional crystallization during lithospheric extension. *Journal of Petrology* **35**, 1055–1094.
- Bergantz, G. W. & Dawes, R. (1994). Aspects of magma generation and ascent in continental lithosphere. In Ryan, M. P. (ed.) *Magmatic Systems*. San Diego, CA: Academic Press, pp. 291–312.
- Bohrson, W. A. & Spera, F. J. (2001). Energy-constrained open-system magmatic processes II: application of energy-constrained assimilation–fractional crystallisation (EC-AFC) model to magmatic systems. *Journal of Petrology* **42**, 1019–1041.
- Bohrson, W. A. & Spera, F. J. (2003). Energy-constrained open-system magmatic processes IV: geochemical, thermal and mass consequences of energy-constrained recharge, assimilation and fractional crystallisation (EC-RAFC). *Geochemistry, Geophysics, Geosystems* **4**, doi: 10.1029/2002GC00316.
- Bott, M. H. P. & Tantrigoda, D. A. (1987). Interpretation of the gravity and magnetic anomalies over the Mull Tertiary intrusive complex, NW Scotland. *Journal of the Geological Society, London* **144**, 17–28.
- Bott, M. H. P. & Tucson, J. (1973). Deep structure beneath the Tertiary volcanic regions of Skye, Mull, and Ardnamurchan, north-west Scotland. *Nature, Physical Sciences* **242**, 114–116.
- Bowen, N. L. (1928). *The Evolution of the Igneous Rocks*. Princeton, NJ: Princeton University Press, 334 pp.
- Buist, D. S. (1959). The composite sill of Rubh'an Eireannaich, Skye. *Geological Magazine* **96**, 247–252.
- Carter, S. R., Evensen, N. M., Hamilton, P. J. & O'Nions, K. (1978). Neodymium and strontium isotope evidence for crustal contamination of continental volcanics. *Science* **202**, 743–747.
- Chadwick, R. A. & Pharoah, T. C. (1998). The seismic reflection MOHO beneath the United Kingdom and adjacent areas. *Tectonophysics* **299**, 255–279.
- Chambers, L. M. & Pringle, M. S. (2001). Age and duration of activity at the Isle of Mull Tertiary igneous centre, Scotland, and confirmation of the existence of subchrons during Anomaly 26r. *Earth and Planetary Science Letters* **193**, 333–345.
- Chapman, H. J. & Moorbath, S. (1977). Lead isotope measurements from the oldest recognised Lewisian gneisses of North-west Scotland. *Nature* **268**, 41–42.
- Crisp, J. A. (1984). Rates of magma emplacement and volcanic output. *Journal of Volcanology and Geothermal Research* **20**, 177–211.
- Dagley, P., Mussett, A. E. & Skelhorn, R. R. (1990). Magnetic polarity stratigraphy of the Tertiary rocks of Skye, Scotland. *Geophysical Journal International* **101**, 395–409.

- Dickin, A. P. (1981). Isotope geochemistry of Tertiary igneous rocks from the Isle of Skye, NW Scotland. *Journal of Petrology* **22**, 155–189.
- Dickin, A. P. (1983). Hydrothermal fluid pathways at the contact of the Beinn an Dubhaich Epigranite, Isle of Skye. *Scottish Journal of Geology* **19**, 235–242.
- Dickin, A. P. & Exley, R. A. (1981). Isotopic and geochemical evidence for magma mixing in the petrogenesis of the Coire Uaigneich Granophyre, Isle of Skye, NW Scotland. *Contributions to Mineralogy and Petrology* **76**, 98–108.
- Dickin, A. P., Exley, R. A. & Smith, B. M. (1980). Isotopic measurement of Sr and O exchange between meteoric–hydrothermal fluid and the Coire Uaigneich Granophyre, Isle of Skye, NW Scotland. *Earth and Planetary Science Letters* **51**, 58–70.
- Dickin, A. P., Brown, J. L., Thompson, R. N., Halliday, A. N. & Morrison, M. A. (1984). Crustal contamination and the granite problem in the British Tertiary Volcanic Province. *Philosophical Transactions of the Royal Society of London* **A310**, 755–780.
- Dickin, A. P., Jones, N. W., Thirlwall, M. F. & Thompson, R. N. (1987). A Ce/Nd isotope study of crustal contamination processes affecting Paleocene magmas in Skye, Northwest Scotland. *Contributions to Mineralogy and Petrology* **96**, 455–464.
- Ellam, R. M. (1992). Lithospheric thickness as a control on basalt geochemistry. *Geology* **20**, 153–156.
- Ellam, R. M. & Stuart, F. M. (2000). The sub-lithospheric source of North Atlantic basalts: evidence for, and significance of, a common end-member. *Journal of Petrology* **41**, 919–932.
- Emeleus, C. H. (1982). The central complexes. In Sutherland, D. S. (ed.) *Igneous Rocks of the British Isles*. Chichester: John Wiley, pp. 369–414.
- Emeleus, C. H. (1991). Tertiary igneous activity. In Craig, G. Y. (ed.) *Geology of Scotland*. London: Geological Society, pp. 455–502.
- Emeleus, C. H. & Gyopari, M. C. (1992). *British Tertiary Volcanic Province*. London: Chapman and Hall, 259 pp.
- England, R. W. (1994). The structure of the Skye lava field. *Scottish Journal of Geology* **30**, 33–37.
- Ferry, J. M. (1985). Hydrothermal alteration of Tertiary igneous rocks from the Isle of Skye, northwest Scotland II. Granites. *Contributions to Mineralogy and Petrology* **91**, 283–304.
- Forrester, R. W. & Taylor, H. P. (1977).  $^{18}\text{O}/^{16}\text{O}$ , D/H,  $^{13}\text{C}/^{12}\text{C}$  studies of the Tertiary igneous complex of Skye, Scotland. *American Journal of Science* **277**, 136–177.
- Gass, I. G. & Thorpe, R. S. (1976). Igneous case study: the Tertiary igneous rocks of Skye, NW Scotland. In Aprahamian, F. (ed.) *Science: A Third Level Course. Earth Science Topics and Methods*. Milton Keynes: Open University Press.
- Geldmacher, J., Troll, V. R., Emeleus, C. H. & Donaldson, C. H. (2002). Pb isotope evidence for contrasting crustal contamination of primitive to evolved magmas from Ardnamurchan and Rum: implications for the structure of the underlying crust. *Scottish Journal of Geology* **38**, 55–61.
- Ghiorso, M. S. (1997). Thermodynamic models of igneous processes. *Annual Review of Earth and Planetary Sciences* **25**, 221–241.
- Gibb, F. G. F. & Gibson, S. A. (1989). The Little Minch Sill Complex. *Scottish Journal of Geology* **3**, 367–370.
- Gibson, S. A. (1988). The geochemistry, mineralogy and petrology of the Trotternish Sill Complex, northern Skye, Scotland. Ph.D. thesis, Kingston Polytechnic.
- Gibson, S. A. (1990). The geochemistry of the Trotternish sills, Isle of Skye: crustal contamination in the British Tertiary Volcanic Province. *Journal of the Geological Society, London* **147**, 1071–1081.
- Gibson, S. A. & Jones, A. P. (1991). Igneous stratigraphy and internal structure of the Little Minch Sill Complex, Trotternish Peninsula, northern Skye. *Geological Magazine* **128**, 51–66.
- Gouly, N. R., Leggett, M., Douglas, T. & Emeleus, C. H. (1992). Seismic reflection test on the granite of the Skye Tertiary igneous centre. *Geological Magazine* **129**, 633–636.
- Hamilton, M. A., Pearson, D. G., Thompson, R. N., Kelley, S. P. & Emeleus, C. H. (1998). Rapid eruption of Skye lavas inferred from precise U–Pb and Ar–Ar dating of the Rum and Cuillin plutonic complexes. *Nature* **394**, 260–263.
- Harker, A. (1904). The Tertiary rocks of Skye. *Memoir of the Geological Society of Scotland*, 481 pp.
- Hawkesworth, C. J. & Morrison, M. A. (1978). A reduction in  $^{87}\text{Sr}/^{86}\text{Sr}$  during basalt alteration. *Nature* **276**, 381–383.
- Hildreth, W. & Moorbath, S. (1988). Crustal contributions to arc magmatism in the Andes of Central Chile. *Contributions to Mineralogy and Petrology* **98**, 455–489.
- Holden, P., Halliday, A. N. & Stephens, W. E. (1987). Neodymium and strontium isotope content of microdiorite enclaves points to a mantle input into granitoid production. *Nature* **330**, 53–56.
- Hutchison, R. & Bevan, J. C. (1977). The Cuillin layered igneous complex—evidence for multiple intrusion and former presence of a picritic liquid. *Scottish Journal of Geology* **13**, 197–209.
- Moorbath, S. & Bell, J. D. (1965). Strontium isotope abundance studies and rubidium–strontium age determinations on Tertiary igneous rocks from the Isle of Skye, northwest Scotland. *Journal of Petrology* **6**, 37–66.
- Moorbath, S. & Thompson, R. N. (1980). Strontium isotope geochemistry and petrogenesis of the Early Tertiary lava pile of the Isle of Skye, Scotland, and other basic rocks of the British Tertiary Province: an example of magma–crust interaction. *Journal of Petrology* **21**, 295–321.
- Moorbath, S. & Welke, H. (1969). Lead isotope studies on igneous rocks from the Isle of Skye, northwest Scotland. *Earth and Planetary Science Letters* **5**, 217–230.
- Mussett, A. E., Dagley, P. & Skelhorn, R. R. (1988). Time and duration of activity in the British Tertiary Igneous Province. In Morton, A. C. & Parson, L. M. (eds) *Early Tertiary Volcanism and the Opening of the North Atlantic*. Geological Society, London, *Special Publications* **39**, 337–348.
- Nicolis, G. & Prigogine, I. (1977). *Self-Organisation in Nonequilibrium Systems*. New York: John Wiley, 499 pp.
- Pankhurst, R. J. & Beckinsale, R. D. (1979). Rare earth evidence for the petrogenesis of Tertiary Mull lavas. *Journal of the Geological Society, London* **137**, 112.
- Petford, N. & Gallagher, K. (2001). Partial melting of mafic (amphibolitic) lower crust by periodic influx of basaltic magma. *Earth and Planetary Science Letters* **193**, 483–499.
- Saunders, A. D., Fitton, J. G., Kerr, A. C., Norry, M. J. & Kent, R. W. (1997). The North Atlantic Igneous Province. In Mahoney, J. J. & Coffin, M. F. (eds) *Large Igneous Provinces: Continental, Oceanic, and Planetary Volcanism*. *Geophysical Monograph, American Geophysical Union* **100**, 45–93.
- Scarrow, J. H. (1992). Petrogenesis of the Tertiary lavas of the Isle of Skye, NW Scotland. Ph.D. thesis, University of Oxford.
- Scarrow, J. H. & Cox, K. (1995). Basalts generated by decompressive adiabatic melting of a mantle plume: a case study from the Isle of Skye, NW Scotland. *Journal of Petrology* **36**, 3–22.
- Spera, F. J. (2000). Physical properties of magmas. In: Sigurdsson, H. (ed.) *Encyclopedia of Volcanoes*. New York: Academic Press, pp. 171–190.
- Spera, F. J. & Bohrsen, W. A. (2001). Energy-constrained open-system magmatic processes I: general model and energy-constrained assimilation–fractional crystallisation (EC-AFC) formulation. *Journal of Petrology* **42**, 999–1018.
- Spera, F. J. & Bohrsen, W. A. (2002). Energy-constrained open-system magmatic processes III: energy-constrained recharge, assimilation,

- and fractional crystallisation (EC-RAFC). *Geochemistry, Geophysics, Geosystems* **3**, doi: 10.1029/2002GC00315.
- Spera, F. J. & Bohron, W. A. (2004). Open-system magma chamber evolution: an energy-constrained geochemical model incorporating the effects of concurrent eruption, recharge, variable assimilation, and fractional crystallization. *Journal of Petrology* **45**, in press.
- Stuart, F. M., Ellam, R. M., Harrop, P. J., Fitton, J. G. & Bell, B. R. (2000). Constraints on mantle plumes from the helium isotopic compositions of basalts from the British Tertiary Igneous Province. *Earth and Planetary Science Letters* **117**, 273–285.
- Tantrigoda, D. A. (1988). Interpretation of magnetic anomalies over the Skye Tertiary intrusive complex. *Scottish Journal of Geology*, **24**, 215–221.
- Taylor, H. P. & Forrester, R. W. (1971). Low-O<sup>18</sup> rocks from the intrusive complexes of Skye, Mull, and Ardnamurchan, Western Scotland. *Journal of Petrology* **12**, 465–497.
- Thirlwall, M. F. & Jones, N. W. (1983). Isotope geochemistry and contamination mechanics of Tertiary lavas from Skye, Northwest Scotland. In Hawkesworth, C. J. & Norry, M. J. (eds) *Continental Basalts and Mantle Xenoliths*. Nantwich: Shiva, pp. 186–250.
- Thompson, R. N. (1969). Tertiary granites and associated rocks of the Marsco area, Isle of Skye. *Journal of the Geological Society, London* **124**, 349–385.
- Thompson, R. N. (1972). Evidence for a chemical discontinuity near the basalt–‘andesite’ transition in many anorogenic volcanic suites. *Nature* **236**, 106–110.
- Thompson, R. N. (1974). Primary basalts and magma genesis. *Contributions to Mineralogy and Petrology* **45**, 317–341.
- Thompson, R. N. (1980). Askja 1875, Skye 56 Ma: Basalt triggered plinian, mixed magma eruptions during the emplacement of the Western Redhills granites, Isle of Skye, Scotland. *Geologische Rundschau* **69**, 245–262.
- Thompson, R. N. (1981). Thermal aspects of the origin of the Hebridean Tertiary acid magmas, 1. An experimental study of partial fusion of Lewisian gneisses and Torridonian sediments. *Mineralogical Magazine* **44**, 161–170.
- Thompson, R. N. (1982). Geochemistry and magma genesis. In: Sutherland D. S. (ed.) *The Igneous Rocks of the British Isles*. Chichester: John Wiley, pp. 461–477.
- Thompson, R. N. (1983). Thermal aspects of the origin of Hebridean Tertiary acid magmas; II, Experimental melting behaviour of the granites at 1 kbar P (H<sub>2</sub>O). *Mineralogical Magazine* **47**, 111–121.
- Thompson, R. N., Esson, J. & Dunham, A. C. (1972). Major element chemical variation in the Eocene lavas of the Isle of Skye, Scotland. *Journal of Petrology* **13**, 219–253.
- Thompson, R. N., Gibson, I. L., Marriner, G. F., Matthey, D. P. & Morrison, M. A. (1980). Trace-element evidence of multi-stage mantle fusion and polybaric fractional crystallisation in the Paleocene lavas of Skye, NW Scotland. *Journal of Petrology* **21**, 265–293.
- Thompson, R. N., Dickin, A. P., Gibson, I. L. & Morrison, M. A. (1982). Elemental fingerprints of isotopic contamination of Hebridean Paleocene mantle-derived magmas by Archean sial. *Contributions to Mineralogy and Petrology* **79**, 159–168.
- Thompson, R. N., Morrison, M. A., Dickin, A. P., Gibson, I. L. & Harmon, R. S. (1986). Two contrasting styles of interaction between basic magmas and continental crust in the British Tertiary Igneous Province. *Journal of Geophysical Research* **91**(B6), 5985–5997.
- Tilley, C. E. & Muir, I. D. (1962). The Hebridean Plateau Magma Type. *Transactions of the Edinburgh Geological Society* **19**, 208–215.
- Vogel, T. A., Younker, L. W., Wilband, J. T. & Kampmueller, E. (1984). Magma mixing: the Marsco Suite, Isle of Skye, Scotland. *Contributions to Mineralogy and Petrology* **87**, 231–241.
- Wager, L. R. & Brown, G. M. (1968). *Layered Igneous Rocks*. Edinburgh: Oliver and Boyd, 588 pp.
- Wager, L. R., Weedon, D. S. & Vincent, E. A. (1953). A granophyre from Coire Uaigneich, Isle of Skye, containing quartz paramorphs after tridymite. *Mineralogical Magazine* **30**, 263–276.
- Wager, L. R., Vincent, E. A. & Brown, G. M. (1965). Marscoite and related rocks from the Western Red Hills complex, Isle of Skye. *Philosophical Transactions of the Royal Society of London* **A257**, 273–307.
- Walker, G. P. L. (1993). Basaltic-Volcano Systems. In: Prichard, H. M., Alabaster, T., Harris, N. B. W. & Neary, C. R. (eds) *Magmatic Processes and Plate Tectonics*. London: Geological Society of London, pp. 3–38.
- Walsh, J. N., Beckinsale, R. D., Skelhorn, R. R. & Thorpe, R. S. (1979). Geochemistry and petrogenesis of Tertiary granitic rocks from the Island of Mull, Northwest Scotland. *Contributions to Mineralogy and Petrology* **71**, 99–116.
- Weaver, B. L. & Tarney, J. (1980). Rare earth geochemistry of Lewisian granulite-facies gneisses, northwest Scotland: implications for the petrogenesis of the Archean lower crust. *Earth and Planetary Science Letters* **51**, 279–296.
- Weaver, B. L. & Tarney, J. (1981). Lewisian gneiss geochemistry and Archean crustal development models. *Earth and Planetary Science Letters* **55**, 171–180.
- White, R. S. & McKenzie, D. (1995). Mantle plumes and flood basalts. *Journal of Geophysical Research, B, Solid Earth and Planets* **100**, 17543–17585.
- White, S. M., Spera, F. J. & Crisp, J. A. (2003). Long-term rates of mafic magma emplacement and implications for heat advection. EOS Transactions, American Geophysical Union, **84**, Fall Meeting Supplement, Abstract V12C-0599.
- Whitehouse, M. J. (1990). Isotopic evolution of the southern Outer Hebridean Lewisian gneiss complex: constraints on Late Archean source regions and the generation of transposed Pb–Pb paleo-isochrons. *Chemical Geology* **86**, 1–20.
- Williamson, I. T. & Bell, B. R. (1994). The Paleocene lava field of west–central Skye, Scotland: stratigraphy, paleogeography and structure. *Transactions of the Royal Society of Edinburgh: Earth Sciences* **85**, 39–75.
- Wood, D. A. (1980). The application of the Th–Hf–Ta diagram to problems of tectonomagmatic classification and to establishing the nature of crustal contamination of basaltic lavas of the British Tertiary Volcanic Province. *Earth and Planetary Science Letters* **50**, 11–30.

